Targeting Peptidylarginine Deiminases in Neurons and Astrocytes in Central Nervous System Injury—Pro-Regenerative Effects of Cl-Amidine in an Oxygen-Glucose Deprivation Model of Ischaemia (OGD/R) In Vitro

Dina Ahmed , Stephen J. Getting , Maria Ashioti , Sigrun Lange *

Posted Date: 27 April 2026

doi: 10.20944/preprints202604.1848.v1

Keywords: peptidylarginine deiminases (PADs); deimination/citrullination; central nervous system (CNS); neuron; astrocyte; hypoxia; ischaemia; oxygen-glucose deprivation; Cl-amidine; regeneration

 doi:10.20944/preprints202604.1848.v1

Article

Targeting Peptidylarginine Deiminases in Neurons and Astrocytes in Central Nervous System Injury—Pro-Regenerative Effects of Cl-Amidine in an Oxygen-Glucose Deprivation Model of Ischaemia (OGD/R) In Vitro

Dina Ahmed, Stephen J. Getting, Maria Ashioti and Sigrun Lange *

School of Life Sciences, College of Liberal Arts and Sciences, University of Westminster, 115 New Cavendish Street, London W1W 6UW, UK

* Correspondence: s.lange@westminster.ac.uk

Abstract

Peptidylarginine deiminases (PADs) are a family of five isozymes (PAD1-4, PAD6) in humans, with PAD2, 3 and 4 associated with the central nervous system. PAD mediated post-translational citrullination/deimination of target proteins contributes to pathobiological processes, including in the CNS, where the potential of PAD inhibitor treatment has been reported. This study aimed to identify PAD-dependent pro-regenerative responses in neuronal and astrocytic cells respectively, using human cellular in vitro models to assess the therapeutic effects of pan-PAD, PAD2- and PAD4-isozyme specific inhibitors in an oxygen-glucose deprivation/reperfusion model of ischaemia (OGD/R) at different time windows (30 min, 1 h and 4 h) in conjunction with scratch injury and LPS stimulation. Key findings suggest that pan-PAD inhibitor Cl-amidine promotes CNS regeneration through enhancing wound healing of both neuronal and astrocytic cells, including with a significant inhibition of PAD2 and PAD3 in the neuronal cells, while protective effects in the astrocytic cells indicate involvement of PAD2 and PAD4. Histone H3 citrullination was significantly reduced in response to Cl-amidine treatment in both cell types, indicating changes in epigenetic regulation and immune-responses via NETosis in CNS injury. Cl-amidine treatment modulated key neuronal (beta-3 tubulin) and astrocytic (GFAP) markers and significantly reduced inflammatory cytokine IL-6 levels in astrocytes following 4 h OGD/R in conjunction with LPS. This study emphasizes the potential for pharmacological PAD inhibitor treatment in CNS injury, including future PAD3 inhibitor development to target neuronal injury.

Keywords: peptidylarginine deiminases (PADs); deimination/citrullination; central nervous system (CNS); neuron; astrocyte; hypoxia; ischaemia; oxygen-glucose deprivation; Cl-amidine; regeneration

1. Introduction

Acute Central Nervous System (CNS) injuries include cerebral ischaemia (stroke) and traumatic brain injury (TBI). These represent leading causes of global mortalities and debilitation, with TBI affecting almost 69 million people and stroke affecting above 15 million people annually [1]. Other debilitating forms of acute CNS injury include hypoxic-ischemic encephalopathy (HIE), which affects 1-3 per 1000 neonates [2], and spinal cord injury (SCI), which affects over 15 million people globally [3].

There is increasing evidence for critical roles of Peptidylarginine Deiminases (PADs), within the context of CNS pathologies, including acute CNS injuries, neurodegenerative disease and CNS associated cancers [4–20]. PADs constitute a family of five, calcium dependent isozymes in humans, PAD1, PAD2, PAD3, PAD4 and PAD6, which can convert arginine into citrulline in proteins, causing

 doi:10.20944/preprints202604.1848.v1

post-translational deimination/citrullination. Deimination renders the polar arginine residues of target proteins into neutral citrulline, affecting conformation and function of target proteins, generation of neoepitopes which contribute to inflammatory responses, effects on epigenetic regulation via histone citrullination and extracellular trap formation [21–23].

Various models of acute CNS injuries can model implications on neuronal and astrocytic responses [24–29]. Studies in HIE and TBI models have revealed that protein deimination affects multiple brain regions [5,10], and similar observations have been reported in neurodegenerative diseases [16,30]. Pharmacological PAD inhibition, particularly using the pan-PAD inhibitor Cl-amidine, has shown promise in several in vivo animal models of acute CNS injury [4,5,31]. As translation from preclinical in vivo rodent models remains a challenge [32], further dissection of PAD-mediated mechanisms and the potential for pharmacological PAD inhibitors in human CNS injury in vitro systems are of interest to further current understanding of the different PAD isozymes in neuronal and astrocytic responses.

This study utilized human neuronal (Retinoic-Acid differentiated SH-SY5Y) and astrocytic (SVG-P12) cells to assess PAD isozymes and protective effects of PAD inhibitors using an in vitro model of oxygen-glucose deprivation model of ischaemia (OGD/R) in conjunction with scratch injury. The scratch injury is generally considered a well-established in vitro form of mechanical trauma [24,25,28,33] assessing cellular migration and gap closure as a function of wound healing capacity. OGD/R can mimic cerebral ischaemia in vitro by combining glucose and serum-deprivation of the cell cultures while simultaneously incubating them under hypoxic conditions (0.1 or 1% Oxygen) [34], while application of *Escherichia coli* lipopolysaccharide (LPS) is a commonly used agent to mimic neuroinflammation [35].

The current study aimed at assessing pro-regenerative effects of pharmacological PAD inhibition in neuronal and astrocytic cells in vitro, with a focus on the pan-PAD inhibitor Cl-amidine [4,5,36–38], in addition to PAD2 inhibitor AMF-30a [39] and PAD4 inhibitor GSK-199 [40], as studies on these PAD isozyme specific inhibitors in CNS regeneration are lacking.

We hypothesise that PAD inhibitor treatment induces pro-regenerative and anti-inflammatory responses, with differing effects on neuronal and astrocytic cells. Effects on gap closure speed were assessed alongside changes in histone H3 citrullination, indicative of epigenetic regulation and a marker for extracellular trap formation and associated with neuroinflammatory responses [4,5,41]. In the neurons, changes in beta-3-tubulin (neuronal differentiation) and nestin (stemness marker) were assessed, while in the astrocytic cells, changes in Glial Fibrillary Acidic Protein (GFAP) and S100B were evaluated as these play roles in the astroglia response [42–45]. Changes in release of pro-inflammatory cytokines Interleukin-1β (IL-1 β) and Interleukin-6 (IL-6) were also assessed in both cell types as indicative of neuroinflammatory changes [46].

2. Results

2.1. PAD Isozyme Detection Differs in Neuronal and Astrocytic Cells

Figure 1 shows PAD isozyme detection on differentiated SH-SY5Y cells (Figure 1A) and SVG-P12 cells (Figure 1B) using anti-PAD antibodies against all human- expressed PAD isozymes, with the morphology of both cell-lines shown in Figure 1C,D.

The neuronal (differentiated SH-SY5Y) cells showed strong levels of PAD1, PAD2 and PAD3 – detectable both in cytoplasm and nucleus, which aligns with their previously reported positive expression within the human CNS [15]. In the neuronal cells, levels of PAD4 were negligible, while PAD6 detection was interestingly positively co-localised to the nucleus as confirmed by co-localisation with DAPI (nuclear blue, fluorescent stain) (Figure 1A).

In the SVG-P12 cells, PAD 1 showed similar expression to PADs 2 and 3 exhibiting moderate cytoplasmic and nuclear detection. PAD4 showed the strongest levels, aligning with roles for astrocytes in immunity, whilst PAD6 detection was negligible (Figure 1B).

 doi:10.20944/preprints202604.1848.v1

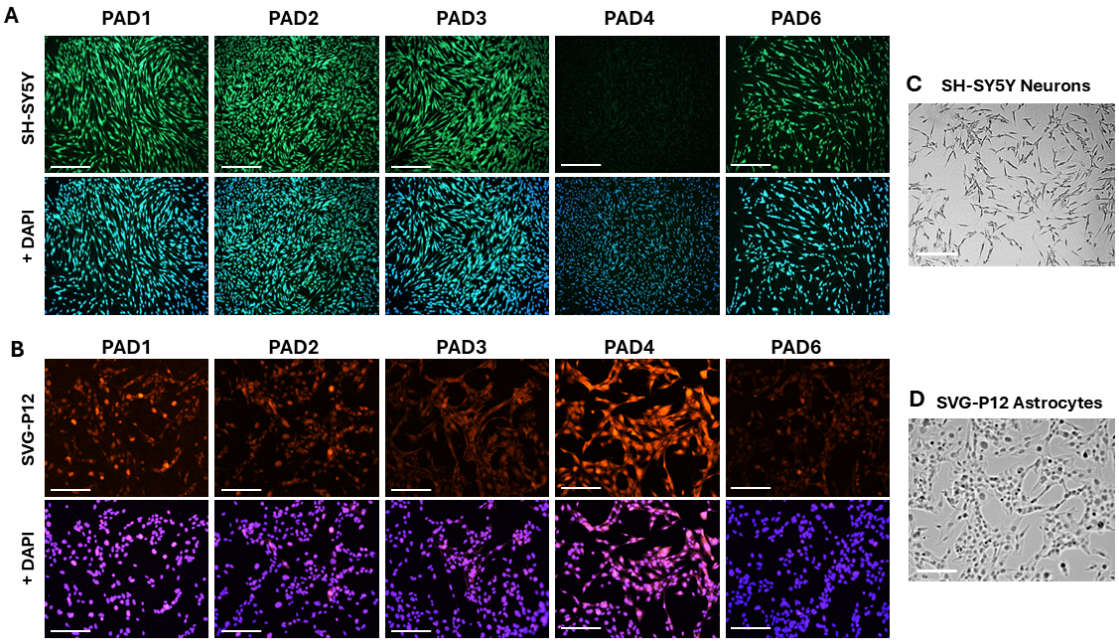

Figure 1. PAD isozyme detection in neurons and astrocytes in vitro. (**A**,**B**) Detection of PAD isozymes (PADs 1-4 and PAD6) by ICC comparing (**A**) neuronal (differentiated SH-SY5Y) and (**B**) astrocytic (SVG-P12) cells, with nuclear DAPI co-staining (blue) shown in parallel. Strong neuronal detection of PADs 1, 2 and 3 was observed, while moderate astrocytic detection was observed, localized both to the cytoplasm and nuclei. PAD4 levels were high in astrocytes, both in cytoplasm and nuclei, but negligible in the neurons. PAD6 showed strong detection with nuclear localization in the neurons, while exhibiting negligible levels in the astrocytes. (**C**) Brightfield images confirming the morphology of differentiated SH-SY5Y cells (neurons) and (**D**) SVG-P12 (astrocytes) cells. The images were taken using EVOS and the 10x objective (scale bar = 275 μm).

2.2. Pharmacological PAD-Inhibition Affects Scratch-Injury Closure in Neuronal and Astrocytic Cells Under Normoxic Conditions

Differentiated SH-SY5Y cells (seeded at 40,000 cells/well) which generated a uniform, confluent, monocellular layer of differentiated cells (Supplementary Figure S1), were exposed to scratch injury followed by application of either 100 μM pan-PAD inhibitor Cl-amidine, 10 μM of PAD2 isozyme specific (AMF-30a) or 5 μM of PAD4 isozyme specific (GSK-199) inhibitors, to assess effects on pan-PAD (including PAD3) inhibition and PAD2 or PAD4 isozyme specific inhibition, respectively.

In all scratch injury experiments, the gap measurement (volume) was assessed at 0 h, 24 h and 48 h post scratch, to assess the effects of PAD inhibitor application, versus control scratch.

Cl-amidine significantly promoted gap closure of the differentiated neurons at 48 h post-scratch (Figure 2A, 2B; n=3). There was no significant change observed for gap closure in response to application of the PAD2 (AMF30a) and PAD4 (GSK199) isozyme specific inhibitors in the neuronal cells (Figure 2B). Assessment of scratch injury in the SVG P12 cells, showed that gap closure was significantly increased by Cl-amidine at 48 h post scratch (Figure 2C,D). Significant effects of the PAD2 and PAD4 isozyme specific inhibitors were not observed on gap closure of the astrocytic cells (Figure 2D).

 doi:10.20944/preprints202604.1848.v1

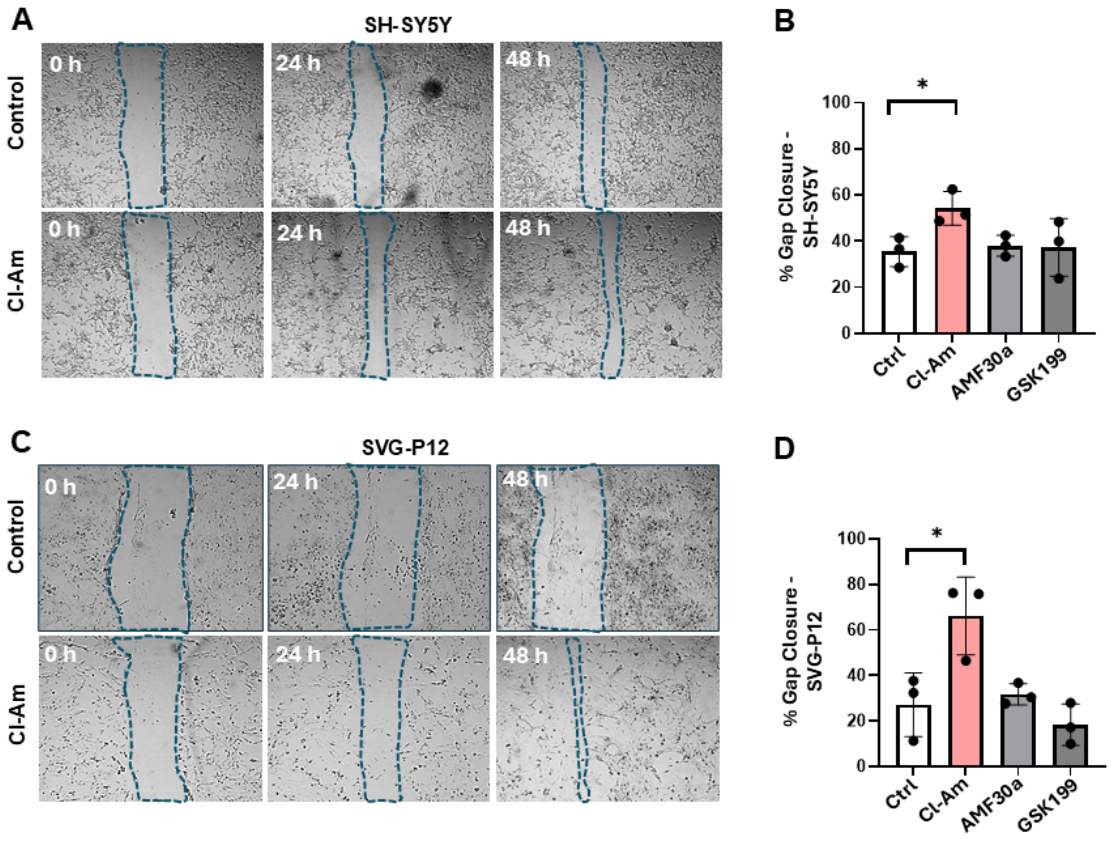

Figure 2. Effects of PAD inhibitors on neuronal and astrocyte cells scratch injured under normoxic incubation with serum and glucose-rich media (**A**) Representative images of wells showing scratch injury (highlighted with the outline) of control untreated, versus Cl-amidine treated neuronal cells. Images captured by EVOS using the 4x objective. (**B**) Bar graph comparing gap closure in control versus Cl-amidine, AMF30a (PAD2 inhibitor) and GSK199 (PAD4 inhibitor) treated neuronal cells, with significant gap closure at the 48 h time-point (t-test, n=3; *$p \leq 0.05$) for Cl-amidine. (**C**) Representative images of wells showing scratch injury (highlighted with the outline) of control untreated, versus Cl-amidine treated astrocytes. Images captured by EVOS using the 4x objective. (**D**) Bar graph comparing gap closure in control versus Cl-amidine, AMF30a and GSK199 treated astrocytes, with significant gap-closure at 48 h post scratch for Cl-amidine (unpaired t-test, n=3; *$p \leq 0.05$).

2.3. Effects of Pan-PAD-Inhibitor on Scratch-Injury of Neuronal Cells and Astrocytes Following OGD/R and LPS Stimulation

Based on the pro-regenerative effects observed with Cl-amidine under normoxia, but negligible effects of the PAD2 (AMF30a) and PAD4 (GSK199) isozyme specific inhibitors, as well as previous studies showing neuroprotective effects for Cl-amidine in acute CNS injury animal models [4,5,31], effects of Cl-amidine in the context of OGD/R and LPS stimulation were next assessed, using the in vitro models of neurons and astrocytes respectively.

Differentiated SH-SY5Y cells were exposed to 30 min, 1 h or 4 h of hypoxic incubation with serum-glucose deprivation in combination with scratch injury to recapitulate OGD/R acute CNS injury (Figure 3).

The scratch injury was furthermore carried out in combination with either 0.1 μg/mL or 1 μg/mL LPS to mimic infection. All the experiments were terminated at 48 h post injury, at which point the gap closure analysis was conducted, based on optimisation of the assay, showing at this point significant and measurable differences between control and treated cells under most of the conditions (Figure 3).

Cl-amidine treated neurons showed significantly faster gap closure under all stress conditions assessed, compared to control wells, at 1 h and 4 h time windows post 4 h OGD/R injury (Figure 3A

 doi:10.20944/preprints202604.1848.v1

– representative images are shown). Pro-regenerative effects of Cl-amidine were observed both for OGD/R alone and also in response to LPS treatment, with more marked effects seen in the cells receiving the higher LPS dose (1 μg/mL) (Figure 3A.3). In the milder 30 min OGD/R model, Cl-amidine exhibited significant neuroprotection when combined with the lower 0.1 μg/mL LPS dose, and a trend showing increased gap closure overall (Figure 3A.1). In the 1 h OGD/R model, Cl-amidine promoted gap-closure of neuronal cells compared with the control non-treated cells (Figure 3A.2). This was also observed in combination with LPS treatment, with significance reached for both LPS doses at 48 h post scratch injury (Figure 3A.2). When using the 30 min OGD/R model, the neuroprotective effects of Cl-amidine were observed as significant when combined with the lower LPS dose (0.1 μg/mL) at 48 h post insult (3A.1).

SVG-P12 cells were exposed to the same conditions as the differentiated neuronal cells and assessed for changes in gap closure following scratch injury as before (Figure 3B,B.1–B.3). Cl-amidine treatment significantly promoted gap closure in the 4 h OGD/R model in combination with LPS stimulation at both doses (Figure 3B,B.1.–B.3). Pro-regenerative effects of Cl-amidine on the astrocytic cells were also observed in the shorter 30 min (Figure 3B.1 and 1 h (Figure 3B.2) OGD/R models, although less pronounced effects were observed for the LPS stimulated wells for those time points (Figure 3B.1–B.3).

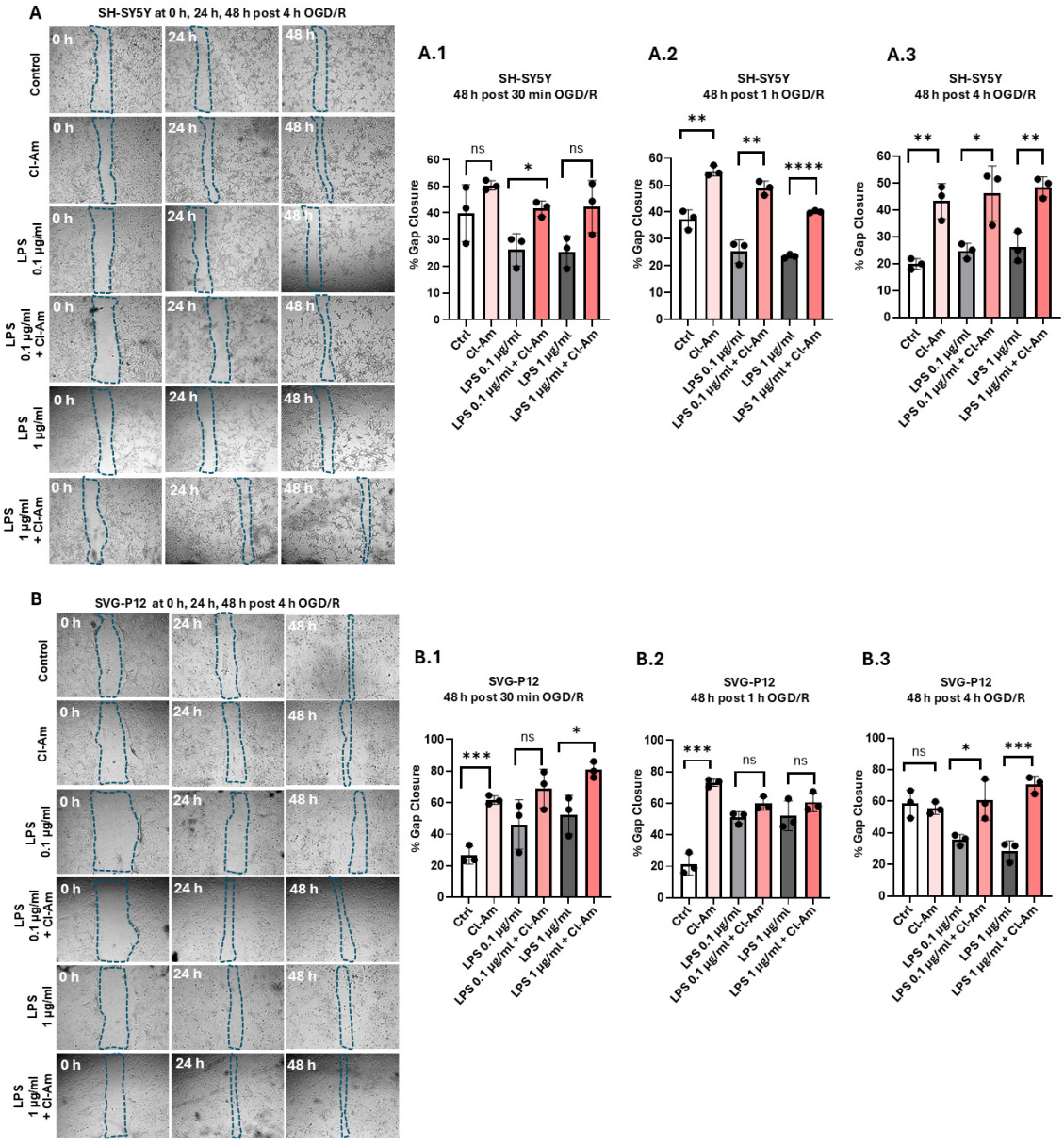

 doi:10.20944/preprints202604.1848.v1

Figure 3. Effects of Cl-amidine on OGD/R scratch injury of neuronal and astrocyte cells exposed to 30 min, 1 h or 4 h hypoxia and LPS stimulation. Scratch assay was carried out in conjunction with exposure to 4 h hypoxia incubation with glucose-serum deprivation (OGD/R) with/without co-infection of either 0.1 or 1 μg/mL LPS and with/without Cl-amidine treatment (100 μM). (**A**) Representative images of scratch injury (highlighted with the outline) gap closure in neuronal (differentiated SH-SY5Y) cells showing Cl-amidine treated versus control wells, for the different conditions (Hypoxia, LPS+Hypoxia) at 4 h post-scratch (images captured by EVOS using the 4x objective). (**A.1–A.3**) Bar graphs represent scratch injury results for neuronal cells exposed to 30 min, 1 h or 4 h hypoxic incubation with glucose-serum deprivation (OGD/R) with/without co-infection with 0.1 or 1 μg/mL LPS and with/without Cl-amidine (100 μM). (n=3, Mean with SD; unpaired t-test, *$p \leq 0.05$, **$p \leq 0.01$, ***$p \leq 0.001$). (**B**) Representative images of gap closure in astrocytes showing Cl-amidine treated versus control wells for the different OGD/R conditions (Hypoxia, LPS+Hypoxia) at 4 h post-scratch (images captured by EVOS using the 4x objective). (**B.1–B.3**) Bar graphs representing scratch injury results for astrocytes exposed to 30 min, 1 h or 4 h hypoxic incubation with glucose-serum deprivation with/without co-infection with 0.1 or 1 μg/mL LPS and with/without Cl-amidine (100 μM). (n=3, Mean with SD; unpaired t-test, *$p \leq 0.05$, **$p \leq 0.01$, ***$p \leq 0.001$).

2.4. Pan-PAD Inhibitor Cl-Amidine Reduces Histone H3 Citrullination (CitH3) in Neuronal and Astrocyte Cells in OGD/R

Protective effects of Cl-amidine to reduce histone H3 citrullination (CitH3) as part of promoting neuronal and astrocytic regeneration were assessed by immunocytochemistry (ICC). Following 4 h OGD/R, Cl-amidine significantly reduced CitH3 detection in the neuronal (differentiated SHSY5Y) cells (Figure 4A), and the same was observed following 30 min OGD/R in the SVG-P12 astrocytes (Figure 4C), both combined with the higher dose (1 μg/mL) of LPS. Figure 4B,D show the quantitative comparative analysis of CitH3 positive detection by ICC, which was significantly reduced within both cell-lines following Cl-amidine treatment under most of the conditions tested: ischaemia, scratch with/without LPS (0.1 μg or 1 μg/mL), along with different intervals (30 min, 1 h or 4 h) of OGD/R (Figure 4B,D). At the 48 h time-point post injury Cl-amidine treated cells showed significantly reduced CitH3 levels by ICC: with representative images shown in Figure 4A,C. Following analysis of all conditions using mean fluorescence intensity, the results showed that Cl-amidine significantly reduced CitH3 levels under most of the conditions applied (Figure 4D).

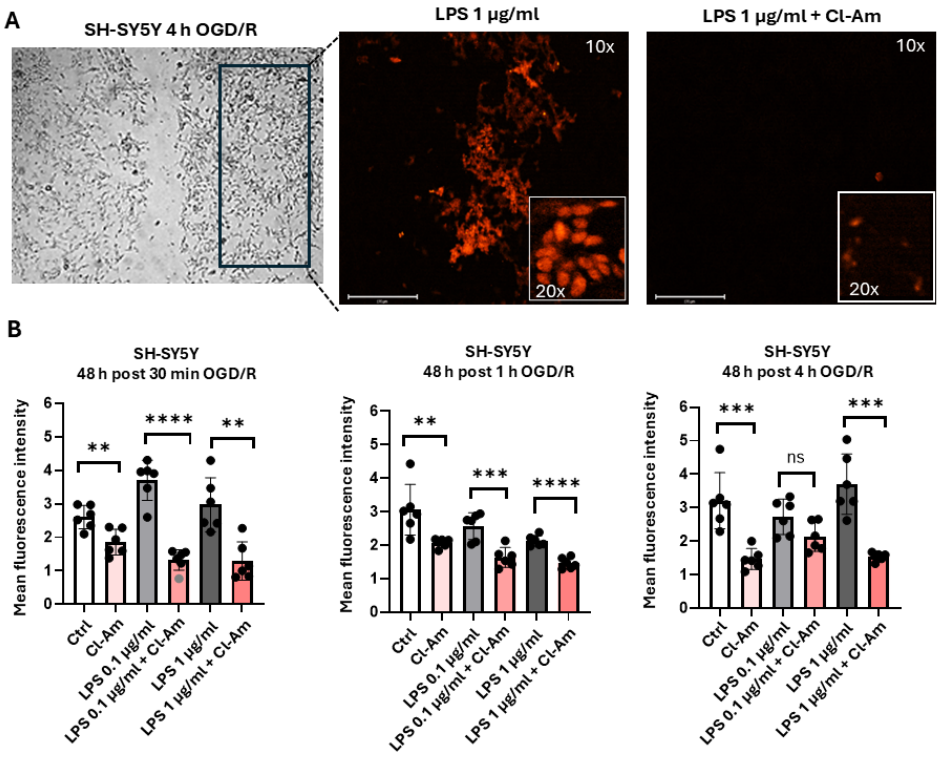

 doi:10.20944/preprints202604.1848.v1

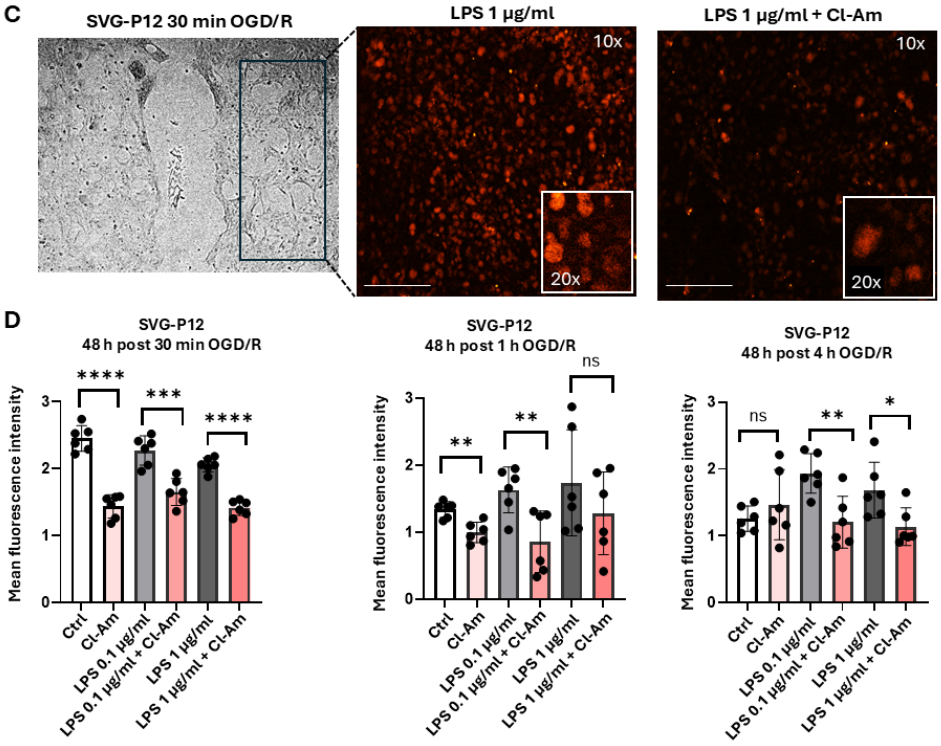

Figure 4. Pan-PAD inhibitor Cl-amidine reduces CitH3 in neuronal and astrocyte cells exposed to scratch injury, hypoxia and LPS stimulation. (**A**) Representative images are shown for Cl-amidine (100 µM), treated neuronal cells exhibiting significantly reduced CitH3 levels (Alexa Fluor red stain) compared to cells not receiving the PAD inhibitor. The cells were exposed to 4 h hypoxic incubation, glucose and serum-deprivation and 1 µg/mL LPS as part of the ischemic, co-infection and scratch injury insult (OGD/R) (Images captured using the 10x objective, adjacent to the scratch injury, with inserted boxes showing higher magnification images at 20x; captured using EVOS). (**B**) Bar charts showing comparative CitH3 levels in neuronal cells as measured by ICC and mean fluorescence intensity (EVOS captured images with the 10x lens, RFP channel). The values were compared between experimental groups using unpaired t-test (n=6, Mean with SD; **$p \leq 0.01$, ***$p \leq 0.001$). (**C**) Effects of Cl-amidine treatment on CitH3 levels in astrocyte (SVG-P12) cells, scratch injured and exposed to ischaemic insult using 30 min hypoxic incubation, glucose and serum- deprivation and 1 µg/mL LPS as part of the ischaemic, co-infection and scratch injury insult (captured with the 10x objective on EVOS; inserted boxes show higher magnification images at 20x). (**D**) Bar charts showing comparative CitH3 levels for SVG-P12 astrocytes (captured with the 10x lens, RFP channel), (n=6, Mean with SD; *$p \leq 0.05$; **$p \leq 0.01$; ***$p \leq 0.001$; ****$p \leq 0.0001$; unpaired t-test comparing control versus respective Cl-am treatment).

2.5. Pan-PAD Inhibitior Modifies Neuronal (β-3-Tubulin), Stemness (Nestin) and Astrocytic (GFAP and S100B) Markers in OGD/R

The results showed that under all conditions, the differentiated SH-SY5Y cells stained strongly for beta-3 tubulin (Figure 5A), confirming their neuronal properties. The changes in staining intensities of beta-3-tubulin were assessed and quantified under all OGD/R conditions at 30 min, 1 h and 4 h; as well as in response to LPS stimulation and Cl-amidine treatment (Figure 5A.1–A.3). In the shorter 30 min model, beta-3 tubulin levels were significantly increased in response to 0.1 µg/mL LPS and reduced in response to Cl-amidine treatment (Figure 5A.1). In the 1 h OGD/R model, a trend was observed for reduced beta-3 tubulin levels in the Cl-amidine treated OGD/R + LPS (0.1 µg/mL) neuronal cells, compared with the LPS stimulation alone (Figure 5A.3). In the 4 h OGD/R model, beta-3 tubulin was elevated in response to Cl-amidine treatment in the LPS treated (0.1 µg/mL) neuronal cells (Figure 5A.3).

Nestin detection was assessed in the neuronal cells as an indicator of stem-ness and the pro-regenerative response (Figure 5B). Nestin levels were significantly decreased in response to Cl-

 doi:10.20944/preprints202604.1848.v1

amidine treatment in the 30 min OGD/R model, with a similar trend observed in combination with the higher LPS dose (1 μg/mL), albeit not statistically significant (Figure 5B.1). In the 1 h OGD/R model, Cl-amidine significantly decreased nestin detection in LPS treated (0.1 μg/mL) neuronal cells (Figure 5B.2), while no significant effects were observed in the other conditions. No significant changes were observed for nestin levels in the 4 h OGD/R experiment (Figure 5B.3).

In the SVG-P12 astrocyte cells, two canonical astrocytic markers, GFAP and S100B, were assessed by ICC under all experimental conditions compared with controls (Figure 5C,D). GFAP detection showed an overlay with the nuclear DAPI staining in the SVG-P12 cells under all conditions (representative image in Figure 5C). Changes in GFAP levels were not statistically significant between treatment groups in the 30 min OGD/R experiment, while there was an observed trend of overall decrease in GFAP positive staining in the Cl-amidine treated groups (Figure 5C.1). In the 1 h OGD/R experiment a statistically significant decrease of GFAP staining was observed for the Cl-amidine treated group in combination with the higher LPS dose, compared with the LPS treatment alone (Figure 5C.2). In the 4 h OGD/R experiment, a significant decrease of GFAP staining was observed in the Cl-amidine treated group in combination with the lower dose of LPS, compared with the LPS treatment alone (Figure 5C.3). When assessing S100B positive staining (Figure 5D), Cl-amidine showed a trend (albeit non-significant) of reducing S100B positive signal in all conditions assessed (Figure 5D.1–D.3), with significant effects observed in the 1 h OGD/R experiment ($p \leq 0.05$), also in conjunction with LPS stimulation at the lower dose ($^{*}p \leq 0.05$) (Figure 5D.2).

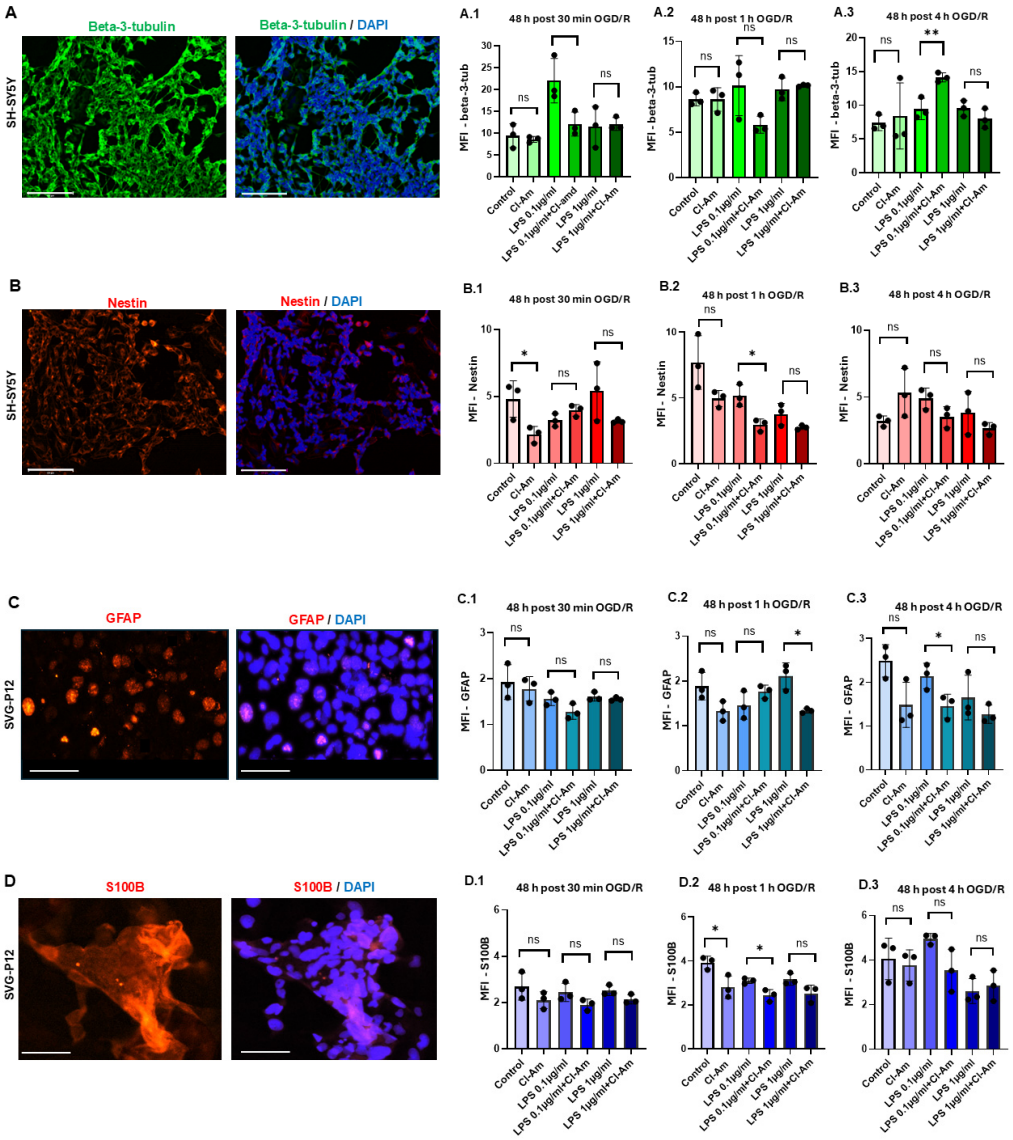

 doi:10.20944/preprints202604.1848.v1

Figure 5. Assessment of neuronal (Beta-3 tubulin) and stem (Nestin) markers in scratch injured neuronal cells, and astrocytic markers (GFAP and S100B) in SVG-P12 cells in OGD/R, and effects of Pan-PAD inhibitor Cl-Amidine. (**A**) Beta-3 tubulin positive staining is strongly detected in neuronal (differentiated SH-SY5Y) cells; examples shown from scratch injured cells exposed to 30 min OGD/R with 0.1 µg/mL LPS stimulation. (**A.1**–**A.3**) Bar charts showing the quantitative analysis (mean fluorescence intensity, MFI) of Beta-3 tubulin staining levels in all conditions at 48 h post 30 min OGD/R (**A.1**), 1 h OGD/R (**A.2**) and 4 h OGD/R (**A.3**) (n=3, Mean with SD; unpaired t-test, *$p \leq 0.05$, **$p \leq 0.01$); (**B**) Nestin detection in differentiated SH-SY5Y cells, indicative of some progenitor-like cells in response to the injury; example shown at 1 h OGD/R + LPS 0.1 µg/mL. (**B.1**–**B.3**) Bar charts showing the quantitative analysis (mean fluorescence intensity, MFI) of Nestin staining levels in all conditions at 48 h post 30 min OGD/R (**B.1**), 1 h OGD/R (**B.2**) and 4 h OGD/R (**B.3**) (n=3, Mean with SD; unpaired t-test, *$p \leq 0.05$). (**C**) GFAP positive staining in SVG-P12 astrocytic cells 48 h post 4 h OGD/R with 0.1 µg/mL LPS co-infection; some nuclear localization of GFAP (red) is detected. (**C.1**–**C.3**) Bar charts showing the quantitative analysis (mean fluorescence intensity, MFI) of GFAP staining levels in all conditions at 48 h post 30 min OGD/R (**C.1**), 1 h OGD/R (**C.2**) and 4 h OGD/R (**C.3**) (n=3, Mean with SD; unpaired t-test, *$p \leq 0.05$). (**D**) S100B detection is shown in SVG-P12 cells scratch injured and exposed to 1 h OGD/R 0.1 µg/mL LPS, at 48 h post injury. (**D.1**–**D.3**). Bar charts showing the quantitative analysis (mean fluorescence intensity, MFI) of S100B staining levels in all conditions at 48 h post 30 min OGD/R (**D.1**), 1 h OGD/R (**D.2**) and 4 h OGD/R (**D.3**) (n=3, Mean with SD; unpaired t-test, *$p \leq 0.05$). All representative images also include the merged images with DAPI and were captured using EVOS using the 20x objective, scale bars = 125 µm.

2.6. Effects of Pan-PAD Inhibitor Cl-Amidine on Pro-Inflammatory Cytokines IL-1β and IL-6 in Neurons and Astrocytes

Effects of Cl-amidine treatment (100 µM) on changes in IL-1β and IL-6 cytokine levels in the neuronal (differentiated SH-SY5Y) and astrocyte (SVG-P12) cells were evaluated by ELISA test at 48 h post 30 min, 1 h and 4 h OGD/R, with and without LPS stimulation (0.1 or 1 µg/mL). Results showed negligible changes in both cytokines in the neuronal cells under all conditions tested (results not shown). In the SVG- P12 cells, no changes were observed for IL-1β, while some differences were observed in the 1 h and 4 h OGD/R groups for IL-6, as presented in Figure 6. After 1 h OGD/R (measured 48 h post insult), LPS stimulation at both doses increased IL-6 levels significantly by approximate 2.5-fold, compared with LPS in control wells, but Cl-amidine addition did not reduce IL-6 levels significantly (Figure 6A). In the 4 h OGD/R model, a significant increase (~3.5 to 5 fold) of IL-6 levels was also observed in combination with OGD/R compared with LPS in control wells and this was significantly reduced (approximately 22%; *$p<0.05$) in response to Cl-amidine treatment in the cells receiving the higher LPS dose (1 µg/mL) (Figure 6B). Cl-amidine treatment in the presence of 0.1 µg/mL LPS reduced IL-6 levels by 14.8% but was not statistically significant (Figure 6B).

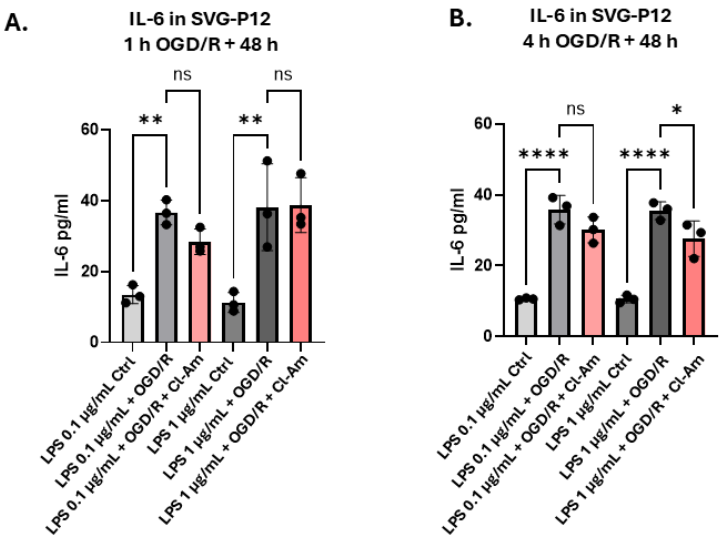

 doi:10.20944/preprints202604.1848.v1

Figure 6. IL-6 detection in SVG-P12 astrocytes using ELISA. (**A**) SVG-P12 cells were exposed to 1 h OGD/R and IL-6 levels measured 48 h post insult. Control wells received LPS (0.1 μg/mL LPS or 1 μg/mL LPS) without OGD/R; treated wells received OGD/R and LPS (0.1 μg/mL LPS or 1 μg/mL LPS) in the presence or absence of Cl-Am (100 mM). (**B**) SVG-P12 cells were exposed to 4 h OGD/R in combination with LPS stimulation (0.1 μg/mL LPS or 1 μg/mL LPS) alone or in combination with Cl-amidine (100 mM). Control wells were not exposed to OGD/R and only treated with LPS. IL-6 levels were determined by ELISA 48 h post insult. Data are represented as mean +/- SD (n=3; *$p \leq 0.05$; **$p \leq 0.01$; ****$p \leq 0.0001$).

3. Discussion

This study assessed roles for PADs in acute CNS injury of OGD/R and neuroinflammation, highlighting the use of in vitro modelling for PADs in human neuronal and astrocyte cell cultures, respectively. The SH-SY5Y neuroblastoma immortalized cell-line was differentiated into neurons using retinoic acid (RA) and has been utilised in various in vitro studies of TBI and ischaemia [47–53]. The astrocyte SVG-P12 cell-line has been used for studying ischaemia [54] and as a control in glioblastoma studies [55,56]. Differences in PAD isozyme levels were detected between the cell lines, with higher detection of PAD3 in neurons, compared with PAD4 in astrocytes, while PAD1 and PAD2 levels were lower in astrocytes than neurons but detectable in both cell lines. This correlates with neuroinflammatory roles for astrocytes in the CNS, including via extracellular trap formation, and possible epigenetic effects on neurons, as indicated by strong CitH3 staining, which can be related to previous findings in animal models, showing elevated CitH3 levels in acute CNS injury [4,5,57]. An unexpected finding was the positive detection of PAD6 in the neuronal cells, as this isozyme is mainly associated with developmental processes [58,59] but aligns with recent reports of PAD6 positive staining in human post-mortem brains samples [15].

The pan-PAD inhibitor Cl-amidine was more effective than the PAD2 and PAD4 isozyme specific inhibitors to promote gap closure in both cell lines, with most marked effects in the 4 h OGD/R insult model. The potential of pharmacologically targeting several PADs to reduce CNS injury correlates with previous in vivo models of spinal cord injury, HIE and TBI showing neuroprotective and pro-regenerative effects for Cl-amidine [4,5,31,60].

In addition to OGD/R, LPS was used to mimic inflammatory responses, and both LPS doses tested (0.1 and 1 μg/mL) correlated with increased levels of CitH3 staining. In macrophages, LPS has been shown to activate PADs and induce CitH3 production in vitro [61]. NETosis is a key player in neuroinflammatory responses [41,62–64] and NETosis inhibition has been shown to improve the overall clinical outcomes post-injury and ischemia [31,65]. Here, Cl-amidine treatment significantly decreased CitH3 levels in both neuronal and astrocytic cells, under all conditions assessed. This correlates to previously reported findings in several in vivo studies assessing CitH3 and NETosis including spinal cord injury, HIE and TBI [4,5,57,66,67].

Some changes in neuronal differentiation (betra-3 tubulin) and stemness (nestin) markers, as well as in astroglial (GFAP and S100B) markers were observed in response to OGD/R and following Cl-amidine treatment.

Beta-3 tubulin constitutes the dynamic end of the cytoskeletal microtubules [68] and was used as a marker of neuronal differentiation for the SH-SY5Y cells. Cl-amidine treatment enhanced neuronal migration following scratch injury, as represented by increased speed of gap closure, in the 1 h and 4 h OGD/R model, with and without LPS. Cl-amidine treatment increased overall beta-3 tubulin levels which aligns with possible roles in promoting neuronal migration [69,70]. Cytoskeletal remodelling via cytoskeletal protein citrullination may be modified, including beta-3 tubulin, which has been previously reported to change in response to PAD inhibitor treatment [68,71]. Our observed effects of Cl-amidine affecting beta-3 tubulin levels may be of considerable importance for CNS protection as the contribution of beta-3 tubulin to neurogenesis and axonal regrowth has been reported in various in vivo neuronal injury and knockout models [72–74]. PAD2-induced citrullination of beta-3 tubulin has for example been shown to be crucial for regulating cytoskeletal

 doi:10.20944/preprints202604.1848.v1

dynamics in murine gonadotropic cells [71]. Further investigations into beta-3 tubulin citrullination must be carried out in future studies.

Nestin, a class VI intermediate filament protein, was used as a marker for neural stem-ness [75–78], to assess possible robust neuro-protective properties following ODG/R and in response to Cl-amidine treatment. Nestin is generally inversely proportional to the level of neuronal differentiation markers [79] and this was observed in the 30 min and 1 h ODG/R models, both with and without LPS, where an increase of beta-3 tubulin coincided with a decrease in nestin levels. The only exception, where both showed increased levels, was in the 4 h OGD/R model in combination with the lower LPS dose (0.1 μg/mL). This aligns with published studies reporting elevated nestin levels in areas of prolonged hypoxic- ischemic insult and injury [80,81]. Our findings indicate that Cl-amidine may exert some neuroprotective effects through elevating nestin in the 4 h OGD/R model. While nestin is known to decline progressively postnatally as the nestin-expressing neural stem cells differentiate, nestin is present in the hippocampal dentate gyrus (DG) and the lateral subventricular zone (SVG), which are brain areas where reactive neurogenesis originates to compensate for neuronal and glial damage post injury and/or insult [82]. Interestingly, nestin is suggested to be a citrullination target similar to other intermediate filaments [83], which may be of interest for future in depth studies.

In the glial cells GFAP levels were significantly decreased in LPS stimulated cells treated with Cl-amidine in the 1 h OGD/R and 4 h OGD/R models. GFAP is a modulator of astrocytic structure and function and upregulated in astrogliosis [84]. S100B levels showed cytoplasmic localisation and a trend for reduced levels in response to Cl-amidine treatment, but only significant in the 1 h OGD/R model in the absence of LPS. S100B is a main contributor to neuronal survival and differentiation along with further numerous cellular activities, most importantly brain tissue repair upon extracellular secretion by the astrocytes [45]. Post brain injury, both GFAP and S100B are considered of clinical relevance, specifically in TBI [45,84,85] where the serum level of both proteins can be directly correlated to the extent of existing brain damage post injury [85]. Moreover, the GFAP is abundant in the blood or any other biological fluid in TBI, SCI or ischaemia indicating neuronal injury, neuroinflammation or neuronal cell death [44,86,87]. While astrogliosis is considered beneficial for initial wound healing, and thus considered neuroprotective, prolonged astrogliosis can impede neuronal regeneration. The results of our study may suggest that Cl-amidine could promote astrocytic gap closure both while decreasing NETosis, as indicative of the reduced CitH3 levels observed, alongside some decrease in GFAP and S100B levels. Interestingly, it was reported that Cl-amidine reduces global citrullination, including GFAP citrullination, in a murine model of retinal gliosis, regulating astrogliosis [88–90]. An interesting observation in the OGD/R model here was that GFAP detection showed similar to reported perinuclear aggregates formed by a *de novo* variant of GFAP-alpha isoform that has been recently reported and linked to juvenile-onset of Alexander disease, a primary astrocytopathy [91]. In the context of ischaemia and LPS stimulation, both promote oxidative stress and enzymatic post-translational modification of cytoskeletal proteins. It can thus be suggested that the detected nuclear signal reflects structurally altered GFAP species with increased solubility and altered intracellular distribution [92–97]. This observed phenomenon may possibly be attributed to cytoskeletal remodelling leading to changes in subcellular localisation under stress conditions and warrants further investigation.

Assessment of the pro-inflammatory cytokines IL-1β and IL-6 by ELISA showed no changes in the neuronal cells, while in the astrocytes a significant increase was observed for IL-6 levels in the 4 h OGD/R model. Furthermore, Cl-amidine treatment significantly decreased elevated IL-6 levels in the presence of LPS (1 μg/mL) stimulation. Several studies using in vivo murine models have reported that IL-6 contributes to the selective activation of astrocytes that underlies their response to CNS injury [90,98–103]. Both in vivo and in vitro studies reported that PAD2 exhibits progressive overexpression in astrocytes undergoing astrogliosis [104–106] and Cl-amidine was shown to reduce IL-6 expression [107]. AS the SVG-P12 cells showed higher levels of PAD4 than PAD2, which coincided with significantly elevated IL-6 levels, a role for PAD4 in addition to PAD2 in IL-6 secretion may be suggested in these cells.

 doi:10.20944/preprints202604.1848.v1

Overall, CNS protective effects of Cl-amidine observed in our study highlight its roles as a potent pan-PAD inhibitor, with the ability to target different and several PAD isozymes depending on their dominance in the cell types, respectively.

4. Materials and Methods

4.1. Cell Culture and Neuronal Cell Differentiation

SH-5Y5Y neuroblastoma cells (ATCC, CRL-2266) were initially cultured in T-75 flasks using complete growth medium comprised of 1:1 DMEM/HAM-F12 medium containing GlutaMax, 10% Fetal Bovine Serum (FBS), 1% penicillin-streptomycin and 1% of non-essential amino acids (NEAA) (Gibco, Fisher Scientific, UK.) in 95% air and 5% CO_2. The medium was changed every 48 h until the cells reached 80% confluence. Thereafter, SH-5Y5Y cells were trypsinised before proceeding to the neuronal differentiation protocol, using 10 μM Retinoic acid (RA) which was supplemented to the complete growth medium to generate a neuronal differentiation medium [108]. The SH-5Y5Y cells were seeded at 25, 30, 40 and 60 x 10^3 cells/well in 24 well plates, to identify optimal seeding density, in the presence of the differentiation medium which was regularly changed every 48 h for a six day period to achieve complete neuronal differentiation; which was confirmed with beta-3 tubulin staining (Supplementary Figure S1). Optimal seeding density was determined as 40 x 10^3 cells/well, and used thereafter. Gentle manual swirling of the plates was carried out to achieve even distribution of the cells across the wells before incubation, to avoid cellular adherence and clustering at the peripheral sides of the walls.

SVG P12 astrocytic cells (ATCC, CRL-8621) were cultured in T-75 flasks using complete growth medium comprised of 1:1 DMEM/HAM-F12 medium containing GlutaMax, 10% FBS, 1% penicillin-streptomycin and 1% NEAA (Gibco Fisher, UK) in 95% air and 5% CO_2. The medium was changed every 24 to 48 h until cells reached 80% confluence. Cells were then trypsinised and seeded at a cell density of 5 x 10^5 cells/well in 24-well plates, according to published optimization for scratch injury experiments [56]. Both cell lines were used at passages 6 to 8.

4.2. Scratch (Wound Healing) Assay

Scratch assay was performed on the differentiated SH-SY5Y cells and the SVG-P12 cells, respectively, using a 200 μL pipette tip to scrape the confluent monolayer of cells longitudinally across the middle of the wells. The culture medium was changed right after the scratch, whereafter either complete medium (control wells, omitting PAD inhibitor) was added or complete medium containing 100 μM pan-PAD inhibitor Cl-amidine (Cayman, No. 10599), 10 μM PAD2 inhibitor AMF30a (CAY10723, Cayman Chemical) or 5 μM PAD4-inhibitor GSK199 (MedChemExpress, 1549811-53-1) for differentiated SH-SY5Y (neurons), where RA was removed before application, and SVG-P12 (astrocytes) cells, depending on the experiment conducted, as further described below.

The cell-migration of both cell lines following scratch injury was determined as percentage of gap closure at 24 h and 48 h (endpoint of the experiments), calculated using the following formula: (A0-At)/A0 x 100; where A0 is the scratched area at time zero and at is the scratched area at 24 h or 48 h, respectively.

4.3. OGD/R in Conjunction with Scratch Injury

To mimic effects of acute CNS injury under ischaemic insult, with/without infection, the following assays were carried out in 24 well plates on both cell lines, proceeding with pan-PAD inhibitor Cl-amidine as this provided the most pro-regenerative effects of the scratch injury in both cell lines under normal conditions: The scratched differentiated SH-SY5Y and SVG-P12 cells were exposed to 30 min, 1 h or 4 h OGD alone or in combination with either 0.1 μg/mL or 1 μg/mL of LPS (from *E. coli* O111:B4; mimicking infection) followed by reperfusion for 48 h. The cells were simultaneously exposed to oxygen and FBS deprivation, using serum-and-glucose free medium,

 doi:10.20944/preprints202604.1848.v1

while for hypoxia, the cells were incubated in a hypoxia chamber (Innova CO-48 incubator, New Brunswick Scientific Co. Inc) adjusted at 95% N_2, 5% CO_2, 0.1% O_2 and 37 °C. Pan-PAD inhibitor Cl-amidine was used at 100 μM concentration (according to [109]) throughout the reperfusion window, using normoxic incubation conditions at 95% O_2, 5% CO_2, and incubated at 37 °C with glucose and serum-enriched media comprising 10% FBS and 17.5 mM of D-Glucose. for assessment of therapeutic outcomes of pan-PAD inhibition following the different time-windows of applied insult, which may inform clinical relevance of PAD inhibitor application post insult. Following reperfusion for 48 h, cells were fixed for Immunocytochemical staining.

4.4. Immunocytochemistry on Differentiated SH-SY5Y and SVG-P12 Cells

Both cell lines were seeded on 24-well plates at a cell density of 40,000 cells/well for differentiated SH-SY5Y cells and at 50,000 cells/well for SVG P12 cells, for immunocytochemical staining of the PAD isozymes (PADs 1-4 and PAD6). Once cells reached 70-80% confluence, the media was removed, and wells were rinsed with PBS-T, 1 mL/well. Scratch injury experiments were furthermore stained for CitH3, beta-3 tubulin, nestin, GFAP and S100B as appropriate.

The cells were fixed with 4% paraformaldehyde in PBS (pH 7.4) for 10 min at room temperature. The cells were thereafter washed 3 x 5 min with ice-cold PBS. Cell permeabilisation was performed for 10 min with PBS containing 0.1% Triton X-100, before washing the cells again three times 5 min with PBS.

Blocking was performed with 1% BSA and 22.52 mg/mL glycine in PBS-T (PBS + 0.1% Tween 20) for 30 min at room temperature, followed by washing with 3 x 5 min in PBS-T. Incubation with primary antibodies was carried out overnight at 4 °C with the following antibody dilutions in PBS-T containing 1% BSA: anti-human PAD1, PAD2, PAD3 and PAD4 (ab181762, ab50257, ab50246, ab50247, Abcam, UK; diluted 1/200), anti-human PAD6 (PA5-72059, Thermo Fisher Scientific; diluted 1/100), CitH3 (ab5103, Abcam; diluted 1/200), Beta-3 tubulin (ab52623, Abcam, diluted 1/500), Nestin (ab18102, Abcam, diluted 1/500), GFAP (ab68428, Abcam, diluted 1/500) and S100B (MA5-42438, Invitrogen-Thermo Fisher Scientific, diluted 1/500) in 1% BSA in PBS-T overnight at 4 °C to make a 100 μL solution in total per well. The negative control wells omitted the primary antibody and were incubated with 1% BSA in PBS-T.

Following primary antibody incubation, the wells were washed 3 x 5 min in PBS, before application of the secondary goat IgG anti-rabbit antibody (Alexa Fluor 488 Abcam ab150077/green or 594 Abcam ab150080/red), except for Nestin, where goat anti-mouse IgG secondary antibody was used (Alexa Fluor 647 Abcam ab150115/red), diluted at 1/500 in 1% BSA in PBS-T for 1 h at RT in the dark, followed by counterstaining with DAPI nuclear stain (Sigma Aldrich, D9542) (1 μg/mL), for 1 min. Imaging was carried out using the EVOS FL Auto Imaging Systems with the respective fluorescent channels for green, red, and DAPI. Corresponding bright field images were captured.

4.5. Assessment of PAD Inhibition on Inflammatory Cytokines IL-1β and IL-6 by ELISA

The differentiated SH-SY5Y neuronal cells and SVG-P12 astrocyte cells were exposed to the different experimental conditions and PAD inhibitor treatment with Cl-amidine, at different time points, as described in the sections above. Commercially available ELISA kits (DY201 and DY206, R&D Systems, Bio-Techne, Abingdon, UK), were used to assess potential changes in pro-inflammatory cytokines IL–1 β and IL–6 in the cell-free supernatants of the cell cultures under the different conditions following manufacturer's instructions and according to previously described methods [110,111]. The commercial ELISA kits show negligible (<1%) cross-reactivity with other cytokines and chemokines according to the manufacturer (R&D systems).

 doi:10.20944/preprints202604.1848.v1

4.6. Statistical Analysis

All experiments were carried out at n=3 or n=6 and data are represented as mean with the error bar showing standard deviation (SD). Student's unpaired t-tests and Bonferroni correction tests were used as appropriate, with significant differences reported as *p<0.05, **p<0.01 and ***p<0.001.

5. Conclusions

In summary, this study highlights important roles for PADs in CNS injury and regeneration, with differential roles of PAD isozymes between neuronal and astrocyte cells. Histone H3 citrullination, indicative of NETosis and epigenetic regulation, was significantly reduced by pan-PAD inhibitor Cl-amidine in both cell types, which correlated with increased healing capacities in our in vitro acute CNS injury model of OGD/R. Findings furthermore highlight roles for PAD3 in neuronal cells, while roles for PAD4 may be more dominant in astrocytes. The findings support other studies on crucial roles for PADs in CNS injury and open the platform for further in-depth assessments of PAD isozyme specific roles and targeted PAD inhibitors in human in vitro models of neuronal injury and repair, including further drug development aimed at PAD3 modulation in CNS injuries.

Supplementary Materials: The following supporting information can be downloaded at the website of this paper posted on Preprints.org, Figure S1: Differentiated SH-SY5Y cells. A. Brightfield shows the differentiated SH-SY5Y cells (following 6 day differentiation with retinoic acid) captured using the 10x and 20x objective; clear neuronal morphology is observed. B. Immunocytochemical staining of the differentiated SH-SY5Y cells showing the nuclear DAPI staining, the positive βIII-tubulin staining as a marker of mature neurons and the merged DAPI/GFP channels. All figures were visualized using the EVOS_FL2 system.

Author Contributions: Conceptualization, D.A. and S.L.; methodology, D.A., S.G., M.A., and S.L.; validation, D.,A., S.G., M.A., and S.L.; formal analysis, D.A., S.G., and S.L.; investigation, D.A., S.G., M.A., and S.L.; resources, D.,A., S.G., M.A., and S.L.; data curation, D.A.; writing—original draft preparation, D.A., and S.L.; writing—review and editing, D.A., S.G., M.A., and S.L. visualization, D,A., S.G., and S.L.; supervision, S.G., M.A., and S.L.; project administration, D.A. and S.L. All authors have read and agreed to the published version of the manuscript.

Funding: This research received no external funding.

Institutional Review Board Statement: Not applicable.

Informed Consent Statement: Not applicable.

Data Availability Statement: The original contributions presented in this study are included in the article/supplementary material. Further inquiries can be directed to the corresponding author.

Acknowledgments: Thanks are due to Prof Dr Khaled Ahmer for support to D.A. through the Egypt Center for Research and Regenerative Medicine.

Conflicts of Interest: The authors declare no conflicts of interest. The funders had no role in the design of the study; in the collection, analyses, or interpretation of data; in the writing of the manuscript; or in the decision to publish the results.

References

1. Pilipović, K.; Harej Hrkać, A.; Kučić, N.; Mršić-Pelčić, J. Modeling Central Nervous System Injury In Vitro: Current Status and Promising Future Strategies. *Biomedicines* **2022**, *11*, 94. https://doi.org/10.3390/biomedicines11010094.
2. Acun, C.; Lavu, R.; Liu, W.; Nicoletti, N.; Ramsey, J.; Aly, H. Therapeutic hypothermia in mild hypoxic ischemic encephalopathy: A clinical dilemma with uncertain long-term outcomes. *Early Hum Dev*. **2026**, *212*, 106427. https://doi.org/10.1016/j.earlhumdev.2025.106427

 doi:10.20944/preprints202604.1848.v1

3. Omelchenko, A.; Singh, N.K.; Firestein, B.L. Current Advances in In Vitro Models of Central Nervous System Trauma. *Curr. Opin. Biomed. Eng.* **2020**, *14*, 34–41. https://doi.org/10.1016/j.cobme.2020.05.002.
4. Lange, S.; Gögel, S.; Leung, K.Y.; Vernay, B.; Nicholas, A.P.; Causey, C.P.; Thompson, P.R.; Greene, N.D.E.; Ferretti, P. Protein Deiminases: New Players in the Developmentally Regulated Loss of Neural Regenerative Ability. *Dev. Biol.* **2011**, *355*, 205–214. https://doi.org/10.1016/j.ydbio.2011.04.015.
5. Lange, S.; Rocha-Ferreira, E.; Thei, L.; Mawjee, P.; Bennett, K.; Thompson, P.R.; Subramanian, V.; Nicholas, A.P.; Peebles, D.; Hristova, M.; Raivich, G. Peptidylarginine Deiminases: Novel Drug Targets for Prevention of Neuronal Damage Following Hypoxic Ischemic Insult (HI) in Neonates**.** *J. Neurochem.* **2014**, *130* (4), 555–562. https://doi.org/10.1111/jnc.12744.
6. Lange, S.; Gallagher, M.; Kholia, S.; Kosgodage, U.S.; Hristova, M.; Hardy, J.; Inal, J.M. Peptidylarginine Deiminases—Roles in Cancer and Neurodegeneration and Possible Avenues for Therapeutic Intervention via Modulation of Exosome and Microvesicle (EMV) Release? *Int. J. Mol. Sci.* **2017**, *18*, 1196. https://doi.org/10.3390/ijms18061196.
7. Lange, S. Peptidylarginine Deiminases as Drug Targets in Neonatal Hypoxic-Ischemic Encephalopathy. ***Front. Neurol.*** **2016**, *7*, 22. https://doi.org/10.3389/fneur.2016.00022.
8. Lange, S. Peptidylarginine Deiminases and Extracellular Vesicles: Prospective Drug Targets and Biomarkers in Central Nervous System Diseases and Repair. *Neural Regen. Res.* **2021**, *16*, 934–938. https://doi.org/10.4103/1673-5374.297058.
9. Stadler, S.C.; Vincent, C.T.; Fedorov, V.D.; Patsialou, A.; Cherrington, B.D.; Wakshlag, J.J.; Mohanan, S.; Zee, B.M.; Zhang, X.; Garcia, B.A.; et al. Dysregulation of PAD4-Mediated Citrullination of Nuclear GSK3β Activates TGF-β Signaling and Induces Epithelial-to-Mesenchymal Transition in Breast Cancer Cells. *Proc. Natl. Acad. Sci. USA* **2013**, *110*, 11851–11856. https://doi.org/10.1073/pnas.1308362110.
10. Lazarus, R.C.; Buonora, J.E.; Jacobowitz, D.M.; Mueller, G.P. Protein Citrullination: A Proposed Mechanism for Pathology in Traumatic Brain Injury. *Front. Neurol.* **2015**, *6*, 204. https://doi.org/10.3389/fneur.2015.00204.
11. Attilio, P.J.; Flora, M.; Kamnaksh, A.; Bradshaw, D.J.; Agoston, D.V.; Mueller, G.P. The Effects of Blast Exposure on Protein Deimination in the Brain. *Oxid. Med. Cell. Longev***.** **2017**, *2017*, 8398072. https://doi.org/10.1155/2017/8398072.
12. Beato, M.; Sharma, P. Peptidyl Arginine Deiminase 2 (PADI2)-Mediated Arginine Citrullination Modulates Transcription in Cancer. *Int. J. Mol. Sci***.** **2020**, *21*, 1351. https://doi.org/10.3390/ijms21041351.
13. Boon, L.; Ugarte-Berzal, E.; Martens, E.; Fiten, P.; Vandooren, J.; Janssens, R.; Blanter, M.; Yu, K.; Boon, M.; Struyf, S.; Proost, P.; Opdenakker, G. Citrullination as a Novel Posttranslational Modification of Matrix Metalloproteinases. *Matrix Biol***.** **2021**, 95, 68–83. https://doi.org/10.1016/j.matbio.2020.10.005.
14. Sancandi, M.; Uysal-Onganer, P.; Kraev, I.; Mercer, A.; Lange, S. Protein Deimination Signatures in Plasma and Plasma-EVs and Protein Deimination in the Brain Vasculature in a Rat Model of Pre-Motor Parkinson's Disease. *Int. J. Mol. Sci.* **2020**, *21*, 2743. https://doi.org/10.3390/ijms21082743.
15. Mercer, A.; Jaunmuktane, Z.; Hristova, M.; Lange, S. Differential, Stage Dependent Detection of Peptidylarginine Deiminases and Protein Deimination in Lewy Body Diseases—Findings from a Pilot Study. *Int. J. Mol. Sci.* **2022**, *23*, 13117. https://doi.org/10.3390/ijms232113117.
16. Mercer, A.; Sancandi, M.; MacLatchy, A.; Lange, S. Brain-Region-Specific Differences in Protein Citrullination/Deimination in a Pre-Motor Parkinson's Disease Rat Model. *Int. J. Mol. Sci.* **2024**, *25*, 11168. https://doi.org/10.3390/ijms252011168.
17. Kosgodage, U.S.; Uysal-Onganer, P.; MacLatchy, A.; Kraev, I.; Chatterton, N.P.; Nicholas, A.P.; Inal, J.M.; Lange, S. Peptidylarginine Deiminases Post-Translationally Deiminate Prohibitin and Modulate Extracellular Vesicle Release and MicroRNAs in Glioblastoma Multiforme. *Int. J. Mol. Sci.* **2019**, *20*, 103. https://doi.org/10.3390/ijms20010103.
18. Uysal-Onganer, P.; MacLatchy, A.; Mahmoud, R.; Kraev, I.; Thompson, P.R.; Inal, J.M.; Lange, S. Peptidylarginine Deiminase Isozyme-Specific PAD2, PAD3 and PAD4 Inhibitors Differentially Modulate Extracellular Vesicle Signatures and Cell Invasion in Two Glioblastoma Multiforme Cell Lines. *Int. J. Mol. Sci.* **2020**, *21*, 1495. https://doi.org/10.3390/ijms21041495.

 doi:10.20944/preprints202604.1848.v1

19. Yusuf, I.O.; Parsi, S.; Ostrow, L.W.; Brown, R.H.; Thompson, P.R.; Xu, Z. PAD2 Dysregulation and Aberrant Protein Citrullination Feature Prominently in Reactive Astrogliosis and Myelin Protein Aggregation in Sporadic ALS. *Neurobiol. Dis.* **2024**, *192*, 106414. https://doi.org/10.1016/j.nbd.2024.106414.
20. Liang, H.; Hunt, J.B., Jr.; Ma, C.; Kovalenko, A.; Calahatian, J.; Pedersen, C.; Liu, H.; Li, J.; Serrano, M.; Blazier, D.; Watler, M.; Rocha-Rangel, P.; Saunders, C.; Blair, L.J.; Breydo, L.; Nash, K.; Quadri, Z.; Kraemer, B.; Nelson, P.; Norris, C.; Abner, E.L.; Uversky, V.N.; Chaput, D.; Selenica, M.B.; Lee, D.C. Probing Tau Citrullination in Alzheimer's Disease Brains and Mouse Models of Tauopathy. *Acta Neuropathol.* **2025**, *150*, 61. https://doi.org/10.1007/s00401-025-02965-5.
21. Bashir, F.; Awais, H.; Waseem, A.; Shahzad, A.; Babar Khan, A.; Ali, S.A.; Shafiq, L.; Ahmed Bhatti, M. Structural and Mechanistic Insights into Peptidylarginine Deiminase (PAD2/PAD4)-Mediated Citrullination and Therapeutic Targeting: A Review. *Int. J. Biol. Macromol*. **2025**, *332*, 148586. https://doi.org/10.1016/j.ijbiomac.2025.148586.
22. Dakin, L.A.; Xing, L.; Hall, J.; Ding, W.; Vajdos, F.F.; Pelker, J.W.; Ramsey, S.; Balbo, P.; Sahasrabudhe, P.V.; Banker, M.E.; Choi, W.Y.; Wright, S.W.; Chang, J.S.; Curto, J.M.; Davoren, J.E.; Drozda, S.E.; Fennell, K.F.; Futatsugi, K.; Kortum, S.; Lee, K.L.; Liu, S.; Lovering, F.; Nicki, J.A.; Trujillo, J.I.; Vincent, F.; Schnute, M.E. Inhibiting Peptidylarginine Deiminases (PAD1-4) by Targeting a Ca2+-Dependent Allosteric Binding Site. *Nat. Commun.* **2025**, 16, 4579. https://doi.org/10.1038/s41467-025-59919-4.
23. Kijak-Boćkowska, M.; Czerwińska, J.; Owczarczyk-Saczonek, A. Peptidylarginine Deiminases: An Overview of Recent Advances in Citrullination Research. *Int. J. Mol. Sci.* **2025**, *26* (24), 12060. https://doi.org/10.3390/ijms262412060.
24. Arun, P.; Abu-Taleb, R.; Valiyaveettil, M.; Wang, Y.; Long, J.B.; Nambiar, M.P. Studies on Blast Traumatic Brain Injury Using In Vitro Model with Shock Tube. *NeuroReport* **2011**, *22*, 379–384. https://doi.org/10.1097/WNR.0b013e328346b138.
25. Hatic, H.; Kane, M.J.; Saykally, J.N.; Citron, B.A. Modulation of Transcription Factor Nrf2 in an In Vitro Model of Traumatic Brain Injury. *J. Neurotrauma* **2012**, *29*, 1188–1196. https://doi.org/10.1089/neu.2011.1806.
26. Bae, Y.-H.; Joo, H.; Bae, J.; Kim, Y.; Lee, H.; Kim, H.; Kim, D.; Kim, K.-S.; Lee, J.; Kim, S. Brain Injury Induces HIF-1α-Dependent Transcriptional Activation of LRRK2 That Exacerbates Brain Damage. *Cell Death Dis*. **2018**, *9*, 1125. https://doi.org/10.1038/s41419-018-1180-y.
27. Chen, W.C.; Chang, L.H.; Huang, S.S.; Huang, Y.J.; Chih, C.L.; Kuo, H.C.; Lee, Y.H.; Lee, I.H. Aryl Hydrocarbon Receptor Modulates Stroke-Induced Astrogliosis and Neurogenesis in the Adult Mouse Brain. *J. Neuroinflammation* **2019**, *16* (1), 187. https://doi.org/10.1186/s12974-019-1572-7.
28. Jing, Y.; Yang, D.; Fu, Y.; Wang, W.; Yang, G.; Yuan, F.; Chen, H.; Ding, J.; Chen, S.; Tian, H. Neuroprotective Effects of Serpina3k in Traumatic Brain Injury. *Front. Neurol.* **2019**, *10*, 1215. https://doi.org/10.3389/fneur.2019.01215.
29. Meyer, L.J.; Lotze, F.P.; Riess, M.L. Simulated Traumatic Brain Injury in In Vitro Mouse Neuronal and Brain Endothelial Cell Culture Models. *J. Pharmacol. Toxicol. Methods* **2022**, *114*, 107159. https://doi.org/10.1016/j.vascn.2022.107159.
30. Gallart-Palau, X.; Lee, B.S.; Adav, S.S.; Qian, J.; Serra, A.; Park, J.E.; Lai, M.K.; Chen, C.P.; Kalaria, R.N.; Sze, S.K. Gender Differences in White Matter Pathology and Mitochondrial Dysfunction in Alzheimer's Disease with Cerebrovascular Disease. *Mol. Brain* **2016**, *9*, 27. https://doi.org/10.1186/s13041-016-0205-7.
31. Shi, G.; Liu, L.; Cao, Y.; Ma, G.; Zhu, Y.; Xu, J.; Zhang, X.; Li, T.; Mi, L.; Jia, H.; Zhang, Y.; Liu, X.; Zhou, Y.; Li, S.; Yang, G.; Liu, X.; Chen, F.; Wang, B.; Deng, Q.; Zhang, S.; Zhang, J. Inhibition of Neutrophil Extracellular Trap Formation Ameliorates Neuroinflammation and Neuronal Apoptosis via STING-Dependent IRE1α/ASK1/JNK Signaling Pathway in Mice with Traumatic Brain Injury. *J. Neuroinflammation* **2023**, *20*, 222. https://doi.org/10.1186/s12974-023-02903-w.
32. Wu, Y.H.; Rosset, S.; Lee, T.R.; Dragunow, M.; Park, T.; Shim, V. In Vitro Models of Traumatic Brain Injury: A Systematic Review. *J. Neurotrauma* **2021**, *38*, 2336–2372. https://doi.org/10.1089/neu.2020.7402.
33. Chen, K.Z.; Liu, S.X.; Li, Y.W.; He, T.; Zhao, J.; Wang, T.; Qiu, X.X.; Wu, H.F. Vimentin as a Potential Target for Diverse Nervous System Diseases. *Neural Regen. Res.* **2023**, *18* (5), 969–975. https://doi.org/10.4103/1673-5374.355744.

 doi:10.20944/preprints202604.1848.v1

34. Liu, Q.; Jin, Z.; Xu, Z.; Yang, H.; Li, L.; Li, G.; et al. Antioxidant Effects of Ginkgolides and Bilobalide against Cerebral Ischemia Injury by Activating the Akt/Nrf2 Pathway In Vitro and In Vivo. *Cell Stress Chaperones* **2019**, *24*, 441–452. https://doi.org/10.1007/s12192-019-00977-1.
35. Skrzypczak-Wiercioch, A.; Sałat, K. Lipopolysaccharide-Induced Model of Neuroinflammation: Mechanisms of Action, Research Application and Future Directions for Its Use. *Molecules* **2022**, *27*, 5481. https://doi.org/10.3390/molecules27175481.
36. Luo, Y.; Arita, K.; Bhatia, M.; Knuckley, B.; Lee, Y.H.; Stallcup, M.R.; Sato, M.; Thompson, P.R. Inhibitors and Inactivators of Protein Arginine Deiminase 4: Functional and Structural Characterization. *Biochemistry* **2006**, *45*, 11727–11736. https://doi.org/10.1021/bi061180d.
37. Wang, Y.; Lyu, Y.; Tu, K.; Xu, Q.; Yang, Y.; Salman, S.; Le, N.; Lu, H.; Chen, C.; Zhu, Y.; Wang, R.; Liu, Q.; Semenza, G.L. Histone Citrullination by PADI4 Is Required for HIF-Dependent Transcriptional Responses to Hypoxia and Tumor Vascularization. *Sci. Adv.* **2021**, *7*, eabe3771. https://doi.org/10.1126/sciadv.abe3771.
38. Ahmed, D.; Puthussery, H.; Basnett, P.; Knowles, J.C.; Lange, S.; Roy, I. Controlled Delivery of Pan-PAD-Inhibitor Cl-Amidine Using Poly(3-Hydroxybutyrate) Microspheres. *Int. J. Mol. Sci. 2021*, *22*, 12852. https://doi.org/10.3390/ijms222312852.
39. Muth, A.; Subramanian, V.; Beaumont, E.; Nagar, M.; Kerry, P.; McEwan, P.; Srinath, H.; Clancy, K.; Parelkar, S.; Thompson, P.R. Development of a Selective Inhibitor of Protein Arginine Deiminase 2. *J. Med. Chem.* **2017**, *60*, 3198–3211. https://doi.org/10.1021/acs.jmedchem.7b00274.
40. Willis, V.C.; Banda, N.K.; Cordova, K.N.; Chandra, P.E.; Robinson, W.H.; Cooper, D.C.; Lugo, D.; Mehta, G.; Taylor, S.; Tak, P.P.; Lewis, H.D.; Holers, V.M. Protein Arginine Deiminase 4 Inhibition Is Sufficient for the Amelioration of Collagen-Induced Arthritis. *Clin. Exp. Immunol.* **2017**, *188*, 263–274. https://doi.org/10.1111/cei.12932.
41. Byun, D.J.; Lee, J.; Yu, J.W.; Hyun, Y.M. NLRP3 Exacerbates NETosis-Associated Neuroinflammation in an LPS-Induced Inflamed Brain. **Immune** *Netw.* **2023**, 23 (3), e27. https://doi.org/10.4110/in.2023.23.e27.
42. Frizzo, J.K.; Tramontina, F.; Bortoli, E.; Gottfried, C.; Leal, R.B.; Lengyel, I.; Donato, R.; Dunkley, P.R.; Gonçalves, C.A. S100B-Mediated Inhibition of the Phosphorylation of GFAP Is Prevented by TRTK-12. *Neurochem. Res.* **2004**, *29*, 735–740. https://doi.org/10.1023/B:NERE.0000018844.51009.40.
43. Guerra, M.C.; Tortorelli, L.S.; Galland, F.; Da Ré, C.; Negri, E.; Engelke, D.S.; Rodrigues, L.; Leite, M.C.; Gonçalves, C.A. Lipopolysaccharide Modulates Astrocytic S100B Secretion: A Study in Cerebrospinal Fluid and Astrocyte Cultures from Rats. ***J. Neuroinflammation*** **2011**, *8*, 128. https://doi.org/10.1186/1742-2094-8-128.
44. Yang, Z.; Wang, K.K. Glial Fibrillary Acidic Protein: From Intermediate Filament Assembly and Gliosis to Neurobiomarker. *Trends Neurosci.* **2015**, *38*, 364–374. https://doi.org/10.1016/j.tins.2015.04.003.
45. Janigro, D.; Mondello, S.; Posti, J.P.; Unden, J. GFAP and S100B: What You Always Wanted to Know and Never Dared to Ask. *Front. Neurol. 2022, 13*, 835597. https://doi.org/10.3389/fneur.2022.835597.
46. Richardson, L.S.; Emezienna, N.; Burd, I.; Taylor, B.D.; Peltier, M.R.; Han, A.; Menon, R. Adapting an Organ-on-Chip Device to Study the Effect of Fetal Sex and Maternal Race/Ethnicity on Preterm Birth Related Intraamniotic Inflammation Leading to Fetal Neuroinflammation. *Am. J. Reprod. Immunol.* **2022**, *88*, e13638. https://doi.org/10.1111/aji.13638.
47. Cuende, J.; Moreno, S.; Bolaños, J.P.; Almeida, A. Retinoic Acid Downregulates Rae1 Leading to APC(Cdh1) Activation and Neuroblastoma SH-SY5Y Differentiation. *Oncogene* **2008**, 27, 3339–3344. https://doi.org/10.1038/sj.onc.1210987.
48. Cheung, Y.T.; Lau, W.K.W.; Yu, M.S.; Lai, C.S.W.; Yeung, S.C.; So, K.F.; Chang, R.C.C. Effects of All-Trans-Retinoic Acid on Human SH-SY5Y Neuroblastoma as In Vitro Model in Neurotoxicity Research. *Neurotoxicology* **2009**, 30, 127–135. https://doi.org/10.1016/j.neuro.2008.11.001.
49. Xie, H.; Hu, L.; Li, G. SH-SY5Y Human Neuroblastoma Cell Line: In Vitro Cell Model of Dopaminergic Neurons in Parkinson's Disease. *Chin. Med. J.* **2010**, *123*, 1086–1092.
50. Skotak, M.; Wang, F.; Chandra, N. An In Vitro Injury Model for SH-SY5Y Neuroblastoma Cells: Effect of Strain and Strain Rate. *J. Neurosci. Methods* **2012**, *205*, 159–168. https://doi.org/10.1016/j.jneumeth.2012.01.001.

 doi:10.20944/preprints202604.1848.v1

51. Filograna, R.; Civiero, L.; Ferrari, V.; Codolo, G.; Greggio, E.; Bubacco, L.; Beltramini, M.; Bisaglia, M. Analysis of the Catecholaminergic Phenotype in Human SH-SY5Y and BE(2)-M17 Neuroblastoma Cell Lines upon Differentiation. *PLoS ONE* **2015**, 10, e0136769. https://doi.org/10.1371/journal.pone.0136769.
52. Elnagar, M.R.; Walls, A.B.; Helal, G.K.; Hamada, F.M.; Thomsen, M.S.; Jensen, A.A. Functional Characterization of α7 Nicotinic Acetylcholine and NMDA Receptor Signaling in SH-SY5Y Neuroblastoma Cells in an ERK Phosphorylation Assay. *Eur. J. Pharmacol.* **2018**, 826, 106–113. https://doi.org/10.1016/j.ejphar.2018.02.047.
53. Juntunen, M.; Hagman, S.; Moisan, A.; Narkilahti, S.; Miettinen, S. In Vitro Oxygen-Glucose Deprivation-Induced Stroke Models with Human Neuroblastoma Cell- and Induced Pluripotent Stem Cell-Derived Neurons. *Stem Cells Int.* **2020**, *2020*, 8841026. https://doi.org/10.1155/2020/8841026.
54. Wan, F.; Jin, L.; Qin, Y.; Zeng, Y. Modulation of Muscarinic Receptors by Anisodine Hydrobromide in Cerebral Ischemia. *Cell. Mol. Biol.* **2023**, *69*, 17–24. https://doi.org/10.14715/cmb/2023.69.11.3.
55. Thakor, F.K.; Wan, K.W.; Welsby, P.J.; Welsby, G. Pharmacological Effects of Asiatic Acid in Glioblastoma Cells under Hypoxia. *Mol. Cell. Biochem.* **2017**, *430*, 179–190. https://doi.org/10.1007/s11010-017-2965-5.
56. Demircan, T.; Yavuz, M.; Kaya, E.; Akgül, S.; Altuntaş, E. Cellular and Molecular Comparison of Glioblastoma Multiform Cell Lines. *Cureus* **2021**, *13*, e16043. https://doi.org/10.7759/cureus.16043.
57. Cao, Y.; Shi, M.; Liu, L.; Zuo, Y.; Jia, H.; Min, X.; Liu, X.; Chen, Z.; Zhou, Y.; Li, S.; Yang, G.; Liu, X.; Deng, Q.; Chen, F.; Chen, X.; Zhang, S.; Zhang, J. Inhibition of Neutrophil Extracellular Trap Formation Attenuates NLRP1-Dependent Neuronal Pyroptosis via STING/IRE1α Pathway after Traumatic Brain Injury in Mice. *Front. Immunol.* **2023,** 14, 1125759. https://doi.org/10.3389/fimmu.2023.1125759.
58. Zhang, T.; Liu, P.; Yao, G.; Zhang, X.; Cao, C. A complex heterozygous mutation in PADI6 causes early embryo arrest: A case report. *Front Genet*. **2023,** *13*, 1104085. https://doi.org/10.3389/fgene.2022.1104085
59. Williams, J.P.C.; Mouilleron, S.; Trapero, R.H.; Bertran, M.T.; Marsh, J.A.; Walport, L.J. Structural Insight into the Function of Human Peptidyl Arginine Deiminase *Comput. Struct. Biotechnol. J*. **2024**, *23*, 3258–3269. https://doi.org/10.1016/j.csbj.2024.08.019.
60. Zhu, Y.; Xu, J.; Chai, Y.; Li, P.; Liu, L.; Zhang, S.; Zhang, J.; Chen, X. Neutrophil Extracellular Traps Aggravate Blood-Brain Barrier Disruption via ZBP1/FSP1-Mediated Ferroptosis after Traumatic Brain Injury. *Fluids Barriers CNS* **2025**, *23*, 2. https://doi.org/10.1186/s12987-025-00739-5.
61. Lai, N.S.; Yu, H.C.; Tung, C.H.; Huang, K.Y.; Huang, H.B.; Lu, M.C. Increased Peptidylarginine Deiminases Expression during the Macrophage Differentiation and Participated Inflammatory Responses. *Arthritis Res. Ther.* **2019**, *21*, 108. https://doi.org/10.1186/s13075-019-1896-9.
62. Chen, Y.; Zhang, H.; Hu, X.; Cai, W.; Ni, W.; Zhou, K. Role of NETosis in Central Nervous System Injury. *Oxid. Med. Cell. Longev*. **2022**, *2022*, 3235524. https://doi.org/10.1155/2022/3235524.
63. Savi, M.; Su, F.; Sterchele, E.D.; Bogossian, E.G.; Demailly, Z.; Baggiani, M.; Casu, G.S.; Taccone, F.S. Targeting NETosis in Acute Brain Injury: A Systematic Review of Preclinical and Clinical Evidence. *Cells* **2024**, *13*, 1553. https://doi.org/10.3390/cells13181553.
64. Qiao, S.; Yuan, J.; Zhang, S.C.; Lu, Y.Y.; Zhou, P.; Xin, T. Neutrophil Extracellular Traps in Central Nervous System Disorders: Mechanisms, Implications, and Emerging Perspective. *Front. Immunol.* **2025**, *16*, 1602336. https://doi.org/10.3389/fimmu.2025.1602336.
65. Seol, S.I.; Oh, S.A.; Davaanyam, D.; Lee, J.K. Blocking Peptidyl Arginine Deiminase 4 Confers Neuroprotective Effect in the Post-Ischemic Brain through Both NETosis-Dependent and -Independent Mechanisms. *Acta Neuropathol. Commun*. **2025**, *13*, 33. https://doi.org/10.1186/s40478-025-01951-y.
66. Zhou, R.; Zhang, T.; Sun, J.; Tan, M.; Li, T.; Yang, T.; Dai, S.S.; Liu, Y.W. Neutrophil Extracellular Traps Aggravate Neutrophil Reverse Transendothelial Migration during Traumatic Brain Injury. *Biochem. Biophys. Res. Commun.* **2025**, *778*, 152387. https://doi.org/10.1016/j.bbrc.2025.152387.
67. Li, A.; Pei, T.W.; Qi, H.; Song, L.B.; Fang, J.; Ding, Z.S.; Chen, T. Study on the Function and Mechanism of Neutrophil Extracellular Traps in Regulating Necroptosis Following Traumatic Brain Injury. *Brain Behav.* **2026**, *16*, e71275. https://doi.org/10.1002/brb3.71275.
68. Wood, L.M.; Moore, J.K. β3 Accelerates Microtubule Plus End Maturation through a Divergent Lateral Interface. *Mol. Biol. Cell* **2025**, *36* (4), ar36. https://doi.org/10.1091/mbc.E24-08-0354.

 doi:10.20944/preprints202604.1848.v1

69. Poirier, K.; Saillour, Y.; Bahi-Buisson, N.; Jaglin, X.H.; Fallet-Bianco, C.; Nabbout, R.; Castelnau-Ptakhine, L.; Roubertie, A.; Attié-Bitach, T.; Desguerre, I.; et al. Mutations in the Neuronal β-Tubulin Subunit TUBB3 Result in Malformation of Cortical Development and Neuronal Migration Defects. *Hum. Mol. Genet.* **2010**, *19*, 4462–4473. https://doi.org/10.1093/hmg/ddq377.
70. Kaverina, I.; Straube, A. Regulation of Cell Migration by Dynamic Microtubules. *Semin. Cell Dev. Biol.* **2011**, *22*, 968–974. https://doi.org/10.1016/j.semcdb.2011.09.017.
71. Quigley, E.B.; DeVore, S.B.; Khan, S.A.; Geisterfer, Z.M.; Rothfuss, H.M.; Sequoia, A.O.; Thompson, P.R.; Gatlin, J.C.; Cherrington, B.D.; Navratil, A.M. GnRH Induces Citrullination of the Cytoskeleton in Murine Gonadotrope Cells. *Int. J. Mol. Sci.* **2024**, *25*, 3181. https://doi.org/10.3390/ijms25063181.
72. Moskowitz, P.F.; Oblinger, M.M. Sensory Neurons Selectively Upregulate Synthesis and Transport of the Beta III-Tubulin Protein during Axonal Regeneration. *J. Neurosci.* **1995**, *15*, 1545–1555. https://doi.org/10.1523/JNEUROSCI.15-02-01545.1995.
73. Latremoliere, A.; Cheng, L.; DeLisle, M.; Wu, C.; Chew, S.; Hutchinson, E.B.; Sheridan, A.; Alexandre, C.; Latremoliere, F.; Sheu, S.H.; et al. Neuronal-Specific TUBB3 Is Not Required for Normal Neuronal Function but Is Essential for Timely Axon Regeneration. *Cell Rep.* **2018**, *24*, 1865–1879.e9. https://doi.org/10.1016/j.celrep.2018.07.029.
74. Puri, D.; Barry, B.J.; Engle, E.C. TUBB3 and KIF21A in Neurodevelopment and Disease. *Front. Neurosci.* **2023**, *17*, 1226181. https://doi.org/10.3389/fnins.2023.1226181.
75. Guo, Y.; Wang, Y.Y.; Sun, T.T.; Xu, J.J.; Yang, P.; Ma, C.Y.; Guan, W.J.; Wang, C.J.; Liu, G.F.; Liu C.Q. Neural Progenitor Cells Derived from Fibroblasts Induced by Small Molecule Compounds under Hypoxia for Treatment of Parkinson's Disease in Rats. *Neural Regen. Res*. **2023**, *18*, 1090–1098. https://doi.org/10.4103/1673-5374.355820.
76. Hartmann, J.; Henschel, N.; Bartmann, K.; Dönmez, A.; Brockerhoff, G.; Koch, K.; Fritsche, E. Molecular and Functional Characterization of Different BrainSphere Models for Use in Neurotoxicity Testing on Microelectrode Arrays. *Cells* **2023**, *12*, 1270. https://doi.org/10.3390/cells12091270.
77. Kim, J.T.; Cho, S.M.; Youn, D.H.; Hong, E.P.; Park, C.H.; Lee, Y.; Jung, H.; Jeon, J.P. Therapeutic Effect of a Hydrogel-Based Neural Stem Cell Delivery Sheet for Mild Traumatic Brain Injury. *Acta Biomater.* **2023**, *167*, 335–347. https://doi.org/10.1016/j.actbio.2023.06.027.
78. Wang, G.; Wang, W.; Zhang, Y.; Gou, X.; Zhang, Q.; Huang, Y.; Zhang, K.; Zhang, H.; Yang, J.; Li, Y. Ethanol Changes Nestin-Promoter Induced Neural Stem Cells to Disturb Newborn Dendritic Spine Remodeling in the Hippocampus of Mice. *Neural Regen. Res.* **2024**, *19*, 416–424. https://doi.org/10.4103/1673-5374.379051.
79. Wilhelmsson, U.; Lebkuechner, I.; Leke, R.; Marasek, P.; Yang, X.; Antfolk, D.; Chen, M.; Mohseni, P.; Lasič, E.; Bobnar, S.T.; Stenovec, M.; Zorec, R.; Nagy, A.; Sahlgren, C.; Pekna, M.; Pekny, M. Nestin Regulates Neurogenesis in Mice through Notch Signaling from Astrocytes to Neural Stem Cells. *Cereb. Cortex* **2019**, *29*, 4050–4066. https://doi.org/10.1093/cercor/bhy284.
80. Gilyarov, A.V. Nestin in Central Nervous System Cells. *Neurosci. Behav. Physiol.* **2008**, *38*, 165–169. https://doi.org/10.1007/s11055-008-0025-z.
81. Xiao, Q.X.; Xue, L.L.; Tan, Y.X.; Huangfu, L.R.; Chen, L.; Zhai, C.Y.; Ma, R.F.; Al-Hawwas, M.; Zhou, H.S.; Wang, T.H.; Zhou, X.F.;
82. Wong, A.; Ghassemi, E.; Yellowley, C.E. Nestin Expression in Mesenchymal Stromal Cells: Regulation by Hypoxia and Osteogenesis. *BMC Vet. Res.* **2014**, *10*, 173. https://doi.org/10.1186/s12917-014-0173-z.
83. Briot, J.; Simon, M.; Méchin, M.-C. Deimination, Intermediate Filaments and Associated Proteins. *Int. J. Mol. Sci.* **2020**, *21*, 8746. https://doi.org/10.3390/ijms21228746.
84. Mafuika, N.S.; Naicker, T.; Harrichandparsad, R.; Lazarus, L. The Potential of Serum S100 Calcium-Binding Protein B and Glial Fibrillary Acidic Protein as Biomarkers for Traumatic Brain Injury. *Transl. Res. Anat.* **2022**, *29*, 100228. https://doi.org/10.1016/j.tria.2022.100228.
85. Vos, P.E.; Jacobs, B.; Andriessen, T.M.; Lamers, K.J.; Borm, G.F.; Beems, T.; Edwards, M.; Rosmalen, C.F.; Vissers, J.L. GFAP and S100B Are Biomarkers of Traumatic Brain Injury: An Observational Cohort Study. *Neurology* **2010**, *75*, 1786–1793. https://doi.org/10.1212/WNL.0b013e3181fd62d2.
86. Agoston, D.V.; Shutes-David, A.; Peskind, E.R. Biofluid Biomarkers of Traumatic Brain Injury. *Brain Inj*. **2017**, *31*, 1195–1203. https://doi.org/10.1080/02699052.2017.1357836.

 doi:10.20944/preprints202604.1848.v1

87. Czeiter, E.; Amrein, K.; Gravesteijn, B.Y.; Lecky, F.; Menon, D.K.; Mondello, S.; Newcombe, V.F.J.; Richter, S.; Steyerberg, E.W.; Vyvere, T.V.; Verheyden, J.; Xu, H.; Yang, Z.; Maas, A.I.R.; Wang, K.K.W.; Büki, A.; CENTER-TBI Participants and Investigators. Blood Biomarkers on Admission in Acute Traumatic Brain Injury: Relations to Severity, CT Findings and Care Path in the CENTER-TBI Study. *EBioMedicine* **2020**, 56, 102785. https://doi.org/10.1016/j.ebiom.2020.102785.
88. Gao, K.; Wang, C.R.; Jiang, F.; Wong, A.Y.K.; Su, N.; Jiang, J.H.; Chai, R.C.; Vatcher, G.; Teng, J.; Chen, J.; Jiang, Y.-W.; Yu, A.C.H. Traumatic Scratch Injury in Astrocytes Triggers Calcium Influx to Activate the JNK/c-Jun/AP-1 Pathway and Switch on GFAP Expression. *Glia* **2013**, 61, 2063–2077. https://doi.org/10.1002/glia.22577.
89. Kesherwani, V.; Tarang, S.; Barnes, R.; Agrawal, S.K. Fasudil Reduces GFAP Expression after Hypoxic Injury. *Neurosci. Lett.* **2014**, *576*, 45–50. https://doi.org/10.1016/j.neulet.2014.05.053.
90. Filous, A.R.; Silver, J. Targeting Astrocytes in CNS Injury and Disease: A Translational Research Approach. *Prog. Neurobiol.* **2016**, *144*, 173–187. https://doi.org/10.1016/j.pneurobio.2016.03.009.
91. Yousaf, M.A.; Scartezzini, A.; Colombo, C.; Bachetti, T.; Sarto, E.; Bella, D.D.; Lorenzi, P.; Tinazzi, M.; Fabrizi, G.M.; Vattemi, G.; Savoia, A. A Novel *De Novo* GFAP Variant Causes a Juvenile-Onset Alexander Disease with Bilateral Vocal Cord Paralysis. *Gene* **2025**, *951*, 149388. https://doi.org/10.1016/j.gene.2025.149388.
92. Rodnight, R.; Gonçalves, C.A.; Wofchuk, S.T.; Leal, R. Control of the Phosphorylation of the Astrocyte Marker Glial Fibrillary Acidic Protein (GFAP) in the Immature Rat Hippocampus by Glutamate and Calcium Ions: Possible Key Factor in Astrocytic Plasticity. *Braz. J. Med. Biol. Res.* **1997**, *30*, 325–338. https://doi.org/10.1590/S0100-879X1997000300005.
93. Herskowitz, J.H.; Seyfried, N.T.; Duong, D.M.; Xia, Q.; Rees, H.D.; Gearing, M.; Peng, J.; Lah, J.J.; Levey, A.I. Phosphoproteomic Analysis Reveals Site-Specific Changes in GFAP and NDRG2 Phosphorylation in Frontotemporal Lobar Degeneration. *J. Proteome Res.* **2010**, *9*, 6368–6379. https://doi.org/10.1021/pr100666c.
94. Sullivan, S.M.; Sullivan, R.K.; Miller, S.M.; Ireland, Z.; Björkman, S.T.; Pow, D.V.; Colditz, P.B. Phosphorylation of GFAP Is Associated with Injury in the Neonatal Pig Hypoxic-Ischemic Brain. *Neurochem. Res.* **2012**, *37*, 2364–2378. https://doi.org/10.1007/s11064-012-0774-5.
95. Snider, N.T.; Omary, M.B. Post-Translational Modifications of Intermediate Filament Proteins: Mechanisms and Functions. *Nat. Rev. Mol. Cell Biol.* **2014**, *15*, 163–177. https://doi.org/10.1038/nrm3753.
96. Battaglia, R.A.; Beltran, A.S.; Delic, S.; Dumitru, R.; Robinson, J.A.; Kabiraj, P.; Herring, L.E.; Madden, V.J.; Ravinder, N.; Willems, E.; Goldman, J.E.; Quinlan, R.A.; Snider, N.T. Site-Specific Phosphorylation and Caspase Cleavage of GFAP Are New Markers of Alexander Disease Severity. *eLife* **2019**, *8*, e47789. https://doi.org/10.7554/eLife.47789.
97. Kanuri, S.H.; Sirrkay, P.J. Deciphering the Structural Biology of GFAP: Connotations of Its Potency in Presaging the Diagnosis for Traumatic Brain Injury and AD. *Neurol. Int.* **2025**, *17*, 134. https://doi.org/10.3390/neurolint17090134.
98. Klein, M.A.; Möller, J.C.; Jones, L.L.; Bluethmann, H.; Kreutzberg, G.W.; Raivich, G. Impaired Neuroglial Activation in Interleukin-6 Deficient Mice. *Glia* **1997**, *19*, 227–233. https://doi.org/10.1002/(sici)1098-1136(199703)19:3<227::aid-glia5>3.0.co;2-w
99. Brunello, A.G.; Weissenberger, J.; Kappeler, A.; Vallan, C.; Peters, M.; Rose-John, S.; Weis, J. Astrocytic Alterations in Interleukin-6/Soluble Interleukin-6 Receptor Alpha Double-Transgenic Mice. *Am. J. Pathol.* **2000**, *157*, 1485–1493. https://doi.org/10.1016/S0002-9440(10)64787-6.
100. Levison, S.W.; Jiang, F.J.; Stoltzfus, O.K.; Ducceschi, M.H. IL-6-Type Cytokines Enhance Epidermal Growth Factor-Stimulated Astrocyte Proliferation. **Glia 2000**, *32*, 328–337. https://doi.org/10.1002/1098-1136(200012)32:3<328::aid-glia110>3.0.co;2-7
101. Okada, S.; Nakamura, M.; Katoh, H.; Miyao, T.; Shimazaki, T.; Ishii, K.; Yamane, J.; Yoshimura, A.; Iwamoto, Y.; Toyama, Y.; Okano., H. Conditional Ablation of Stat3 or Socs3 Discloses a Dual Role for Reactive Astrocytes after Spinal Cord Injury. *Nat. Med.* **2006**, *12*, 829–834. https://doi.org/10.1038/nm1425.
102. Krasovska, V.; Doering, L.C. Regulation of IL-6 Secretion by Astrocytes via TLR4 in the Fragile X Mouse Model. *Front. Mol. Neurosci.* **2018**, *11*, 272. https://doi.org/10.3389/fnmol.2018.00272.

 doi:10.20944/preprints202604.1848.v1

103. Pons-Espinal, M.; Blasco-Agell, L.; Fernandez-Carasa, I.; Andrés-Benito, P.; di Domenico, A.; Richaud-Patin, Y.; Baruffi, V.; Marruecos, L.; Espinosa, L.; Garrido, A.; Tolosa, E.; Edel, M.J.; Otero, M.J.; Mosquera, J.L.; Ferrer, I.; Raya, A.; Consiglio, A. Blocking IL-6 Signaling Prevents Astrocyte-Induced Neurodegeneration in an iPSC-Based Model of Parkinson's Disease. *JCI Insight* **2024**, *9*, e163359. https://doi.org/10.1172/jci.insight.163359.
104. Ishigami, A.; Ohsawa, T.; Hiratsuka, M.; Taguchi, H.; Kobayashi, S.; Saito, Y.; Murayama, S.; Asaga, H.; Toda, T.; Kimura, N.; et al. Abnormal Accumulation of Citrullinated Proteins Catalyzed by Peptidylarginine Deiminase in Hippocampal Extracts from Patients with Alzheimer's Disease. *J. Neurosci. Res.* **2005**, *80*, 120–128. https://doi.org/10.1002/jnr.20431
105. Jang, B.; Jin, J.K.; Jeon, Y.C.; Cho, H.J.; Ishigami, A.; Choi, K.C.; Carp, R.I.; Maruyama, N.; Kim, Y.S.; Choi, E.K. Involvement of Peptidylarginine Deiminase-Mediated Post-Translational Citrullination in Pathogenesis of Sporadic Creutzfeldt-Jakob Disease. *Acta Neuropathol. 2010*, *119*, 199–210. https://doi.org/10.1007/s00401-009-0625-x.
106. Yusuf, I.O.; Qiao, T.; Parsi, S.; Tilvawala, R.; Thompson, P.R.; Xu, Z. Protein Citrullination Marks Myelin Protein Aggregation and Disease Progression in Mouse ALS Models. *Acta Neuropathol. Commun.* **2022**, *10*, 135. https://doi.org/10.1186/s40478-022-01433-5.
107. McNee, G.; Eales, K.L.; Wei, W.; Williams, D.S.; Barkhuizen, A.; Bartlett, D.B.; Essex, S.; Anandram, S.; Filer, A.; Moss, P.A.; Davies, C.C.; Tennant, D.A. Citrullination of Histone H3 Drives IL-6 Production by Bone Marrow Mesenchymal Stem Cells in MGUS and Multiple Myeloma. *Leukemia* **2017**, *31*, 373–381. https://doi.org/10.1038/leu.2016.187.
108. De Conto, V.; Cheung, V.; Maubon, G.; Souguir, Z.; Maubon, N.; Vandenhaute, E.; Bérézowski, V. In Vitro Differentiation Modifies the Neurotoxic Response of SH-SY5Y Cells. *Toxicol.* In Vitro **2021**, *77*, 105235. https://doi.org/10.1016/j.tiv.2021.105235.
109. U, K.P.; Subramanian, V.; Nicholas, A.P.; Thompson, P.R.; Ferretti, P. Modulation of Calcium-Induced Cell Death in Human Neural Stem Cells by the Novel Peptidylarginine Deiminase-AIF Pathway. *Biochim. Biophys. Acta Mol. Cell Res.* **2014**, *1843*, 1162–1171. https://doi.org/10.1016/j.bbamcr.2014.02.018.
110. Kaneva, M.K.; Kerrigan, M.J.; Grieco, P.; Curley, G.P.; Locke, I.C.; Getting, S.J. Chondroprotective and Anti-Inflammatory Role of Melanocortin Peptides in TNF-α Activated Human C-20/A4 Chondrocytes. *Br. J. Pharmacol.* **2012**, *167*, 67–79. https://doi.org/10.1111/j.1476-5381.2012.01968.x.
111. Can, V.C.; Locke, I.C.; Kaneva, M.K.; Kerrigan, M.J.P.; Merlino, F.; De Pascale, C.; Grieco, P.; Getting, S.J. Novel Anti-Inflammatory and Chondroprotective Effects of the Human Melanocortin MC1 Receptor Agonist BMS-470539 Dihydrochloride and Human Melanocortin MC3 Receptor Agonist PG-990 on Lipopolysaccharide Activated Chondrocytes. *Eur. J. Pharmacol.* **2020**, *872*, 172971. https://doi.org/10.1016/j.ejphar.2020.172971.